THE ASTROPHYSICAL JOURNAL, 324:248–266, 1988 January 1

A CO SURVEY OF THE SOUTHERN MILKY WAY: THE MEAN RADIAL DISTRIBUTION OF MOLECULAR CLOUDS WITHIN THE SOLAR CIRCLE

L. BRONFMAN,[1,2,3] R. S. COHEN,[2] H. ALVAREZ,[1] J. MAY,[1] AND P. THADDEUS[2,3,4]

Received 1986 May 7; accepted 1987 March 4

ABSTRACT

The first out-of-plane CO survey of the southern Milky Way has been completed using the Columbia 1.2 m Millimeter-Wave Telescope at Cerro Tololo, Chile, and combined with the Northern CO Survey made with the Columbia Telescope in New York City to provide homogeneous coverage of the inner Galaxy. From these data we derived the mean radial distribution of molecular clouds in the Galactic disk for $R = 2$–10 kpc. About 70% of the molecular gas lies in a well-defined ring, with an inner radius of 4 kpc and an outer radius of 8 kpc. A total H_2 mass of $1.2 \times 10^9\ M_\odot$ has been found for $R = 2$–10 kpc. A separate analysis of the Northern and Southern data shows that, although the mean radius of the distribution (6.5 kpc) and the mean thickness of the molecular disk (70 pc HWHM) are roughly constant from north to south, the radial dependence of the H_2 density distribution changes enough to imply large-scale deviations from azimuthal symmetry.

The Stony Brook/Massachusetts Northern CO survey fit to an axisymmetric model of the molecular Galaxy yields a value of the total H_2 mass 2.2 times larger than ours. This discrepancy has been resolved into three comparable factors: different instrumental calibrations (20%); different proportionality constants to convert CO luminosities into H_2 column densities (30%); and different statistical analyses (40%). Of these two axisymmetric analyses, only ours is self-consistent in that it can reproduce the observed longitudinal distribution of CO intensity integrated in velocity and Galactic latitude, $I(l)$. When compared to the H I mass ($0.9 \times 10^9\ M_\odot$), the present value of the H_2 mass, which is largely free of systematic instrumental errors because the $N(H_2)/W(CO)$ ratio used here was calibrated directly from Columbia CO data, implies a rough equipartition between atomic and molecular hydrogen in the Galactic disk within the solar circle.

Subject headings: galaxies: The Galaxy — interstellar: abundances — interstellar: matter — interstellar: molecules

I. INTRODUCTION

Several large-scale CO surveys from the northern hemisphere have established the gross distribution of molecular clouds in the inner Galaxy over at least a limited part (about one-third) of the area within the solar circle (Scoville and Solomon 1975; Burton *et al.* 1975; Cohen and Thaddeus 1977). Within this region the distribution distinctly peaks about halfway from the Galactic center to the Sun, falling off at the solar circle to a mean cloud density only about one-fourth that at the peak. Between 1 kpc and 3 kpc from the center there is very little CO emission, and so, presumably, little molecular hydrogen, but within 1 kpc of the center there are enormous CO enhancement and evidence of noncircular motions exceeding 150 km s^{-1}. The molecular mass of this enigmatic region is quite poorly known, owing to uncertainty in relating CO intensity to H_2 column density, but it may be as much as half that between 2 kpc and the solar circle, the region studied in the present paper. Beyond the solar circle the molecular mass also is poorly known but almost certainly is only a small fraction of that within.

No large-scale CO survey has covered the fourth quadrant, most of which is too far south to be observed from existing millimeter-wave observatories in the northern hemisphere. Given the deviations from azimuthal symmetry detected by preliminary in-plane observations (Robinson *et al.* 1984; Cohen, Thaddeus, and Bronfman 1985), extrapolation of the northern results to the south is an extremely dubious procedure. With the 1.2 m Chile Telescope at Cerro Tololo, we have now completed the Southern Deep CO Survey, or Southern Survey for short, which covers a thick, strip in Galactic latitude, from $b = -2°$ to 2°, extending from $l = 300°$ to 348° (Fig. 1). This survey is a mirror image in longitude, with improved coverage and sampling in latitude, of the Northern Deep CO Survey, or Northern Survey, made with a similar telescope in New York City (Cohen 1978; Cohen, Dame, and Thaddeus 1986); the two together constitute the first homogeneous and fairly complete inventory of distant molecular clouds in the inner Galaxy. As the initial step in the joint analysis of the two surveys, which sample about 67% of the face-on Galaxy inside the solar circle (Fig. 2), we derived the azimuthally smoothed distribution of molecular clouds and the ratio of molecular to atomic hydrogen between 2 kpc and 10 kpc.

Nearly all derivations of the mass of the molecular clouds in the inner Galaxy are based on either the Northern Survey (Cohen and Thaddeus 1977; Cohen, Tomasevich, and Thaddeus 1979; Cohen *et al.* 1980; Thaddeus and Dame 1984) or the Stony Brook/Massachusetts Survey (Solomon, Sanders, and Scoville 1979; Solomon and Sanders 1980; Sanders, Solomon, and Scoville 1984). It has been deduced from the Columbia data that the amount of molecular gas (mainly H_2) between $R = 2$ kpc and 10 kpc, is about the same as that of atomic gas (H I), while Sanders, Solomon, and Scoville (1984, hereafter SSS) have found that the molecular gas is the more massive by a factor of about 3. Different instrumental cali-

[1] Departamento de Astronomía, Universidad de Chile.
[2] Department of Physics, Columbia University.
[3] Harvard-Smithsonian Center for Astrophysics.
[4] Goddard Institute for Space Studies.

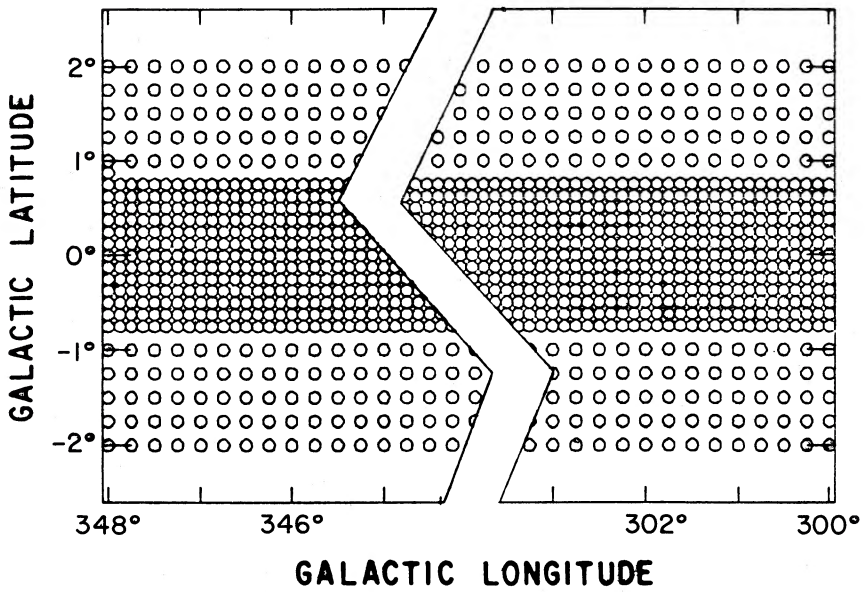

FIG. 1.—Survey sky coverage and sampling. The southern Galactic plane was sampled every 0°.125, (i.e., about every beamwidth) from $b = -0°.75$ to 0°.75, and every 0°.25 beyond.

brations and different adopted ratios of CO integrated intensities to H_2 column densities (Fig. 3) do not fully explain this disagreement. A third factor, previously overlooked, is required: even though essentially the same axisymmetric model of the molecular cloud distribution was used by both the Columbia group and SSS, different procedures were followed to fit the model to the data. Neither analysis, as we shall see, was entirely self-consistent, since neither accurately reproduced the observed doubly-integrated CO intensity, $I(l) = \int T(l, b, v)dvdb$. In the present work we review both previous statistical analyses and derive a new method that accurately predicts $I(l)$, removing the inconsistency in our previous fitting procedure.

The next section (§ II) describes the instrument, the method of data acquisition, and the calibration of the Southern Survey. Observations are presented in § III. In § IV we describe our approach to the axisymmetric analysis, derive the southern CO radial distribution and rederive the northern one, and then compute the H_2 surface density and the total molecular mass in the Galactic disk for $R = 2$–10 kpc. In § V the results of the analysis of the Northern Survey and those of SSS are compared, the differences explained and resolved, and the ratio of H_2 to H I inside the solar circle discussed. We conclude with a summary (§ VI), and in the Appendices discuss further the instrumental calibration (A), describe the statistical treatment of the data (B), which is then compared with previous methods

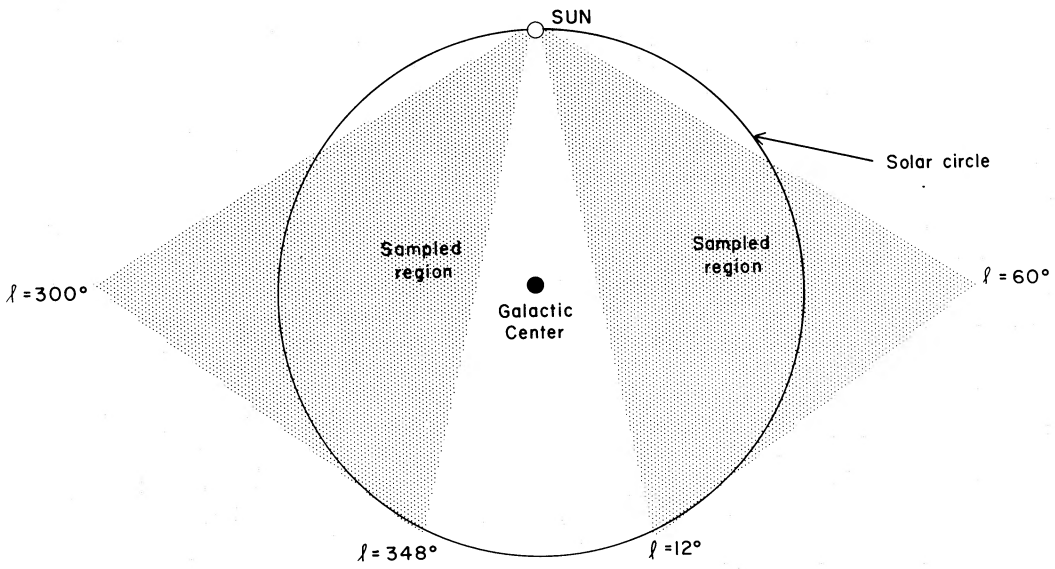

FIG. 2.—Region of the Galactic plane covered by the Columbia Deep CO Surveys

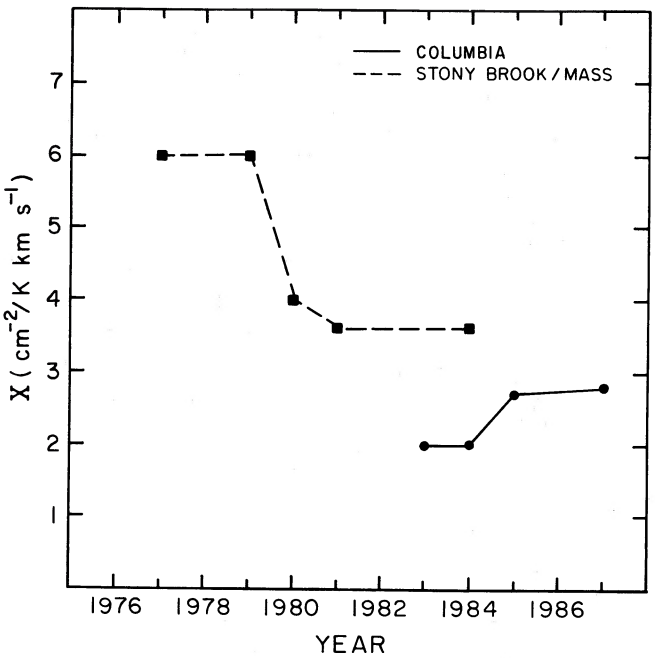

FIG. 3.—Values of the ratio of $N(H_2)$ to $W(CO)$ adopted at Columbia and at Stony Brook/Massachusetts. (Columbia: Dame 1983; Thaddeus and Dame 1984; Dame and Thaddeus 1985; this work. Stony Brook/Massachusetts: Solomon and Sanders 1980 [Conference held in 1977]; Solomon, Sanders, and Scoville 1979; Solomon, Scoville, and Sanders 1979; Sanders 1981; Sanders, Solomon, and Scoville 1984).

(C), and consider the effect on our analysis of a change in Galactic constants $R_\odot$ and $\theta_\odot$ (D).

II. INSTRUMENT AND CALIBRATION

The Columbia Southern Millimeter-Wave Telescope, or Chile Telescope, is a 1.2 m Cassegrain with an effective f/D of 3.79. A close copy of the Columbia Millimeter-Wave Telescope in New York City, it has nearly identical antenna, feed, and calibration. It is housed in an astrodome whose slit is completely covered by a thin screen of Griffolyn, a polyolefin fabric nearly transparent at 2.6 mm, the wavelength of the $1 \rightarrow 0$ rotational transition of CO. The primary, a monolithic aluminum casting purchased from Philco Ford, is diffraction-limited, with a surface accuracy better than $\lambda/100$ at 2.6 mm. The mount can change position by up to 5° in less than 1 s, and hence for position switching can use reference locations well off the Galactic equator in a fast switching cycle of only 30 s. The telescope is small enough to sample well a strip several degrees wide along an entire Galactic quadrant in 1 yr, yet large enough to make a complete inventory of the largest molecular complexes in the inner Galaxy and map the strongest CO sources in the Magellanic Clouds.

The superheterodyne receiver, designed for operation at a remote site, is simple and rugged, but quite sensitive. The first stage, cooled to 77 K by liquid nitrogen, consists of a resonant ring LO diplexer with a signal loss of 0.2 dB, a double-sideband Schottky barrier diode mixer with a noise temperature of 110 K and a conversion loss of 5.2 dB, an impedance matching transformer, and a GaAs FET amplifier operating at the first IF of 1390 MHz. The amplifier has a noise temperature of 15 K and a gain of $\sim$30 dB, constant to 1 dB over a bandwidth of 150 MHz. The second stage, at room temperature, consists of standard commercial components which further amplify the IF signal and convert it to the second IF of 150 MHz sent to the spectrometer. The single-sideband noise temperature of the system is typically 380 K.

By using a liquid nitrogen dewar at 77 K instead of a much more complex and expensive 20 K mechanical refrigerator to cool the first stage of the front end, we achieved most of the benefits of a 20 K receiver while avoiding its disadvantages. During nearly 3 yr of observing, the receiver proved extremely stable, required almost no maintenance, and was easily kept cold for periods as long as 12 months. Its operation was almost as simple as a room-temperature receiver, and its performance approached that of a 20 K one.

As a spectrometer, we used a 256 channel filter bank copied closely from the NRAO design: each channel is 500 kHz wide, for a resolution in radial velocity of 1.3 km s^{-1} at 115 GHz and a spectral range of 333 km s^{-1}, sufficient to cover all the Galactic CO emission at one setting.

The Chile Telescope was assembled early in 1982 on the roof of the Goddard Institute for Space Studies in New York City, where it was fully tested and calibrated before being shipped to the Cerro Tololo Interamerican Observatory (CTIO), arriving there at the end of the year. It began observing within two weeks and has worked since without major instrumental failure. To check the optics, the antenna pattern was measured by means of a transmitter on Cerro Morado, a mountain 3 km away in the antenna's far field (at a distance of about $6D^2/\lambda$). The full width at half-maximum (FWHM) of the main beam was found to be 8.′8, and the first sidelobes were more than 18 dB below the main beam. Cerro Tololo, as expected, proved to be an exceptionally good site for millimeter-wave astronomy, with typical water opacities per air mass of 0.05–0.10, about half that in New York; on average, we worked about 325 days per year, and the weather would probably have permitted more than 345 days of observation.

Spectra were calibrated against a blackbody reference by the standard chopper wheel technique used at other millimeter-wave telescopes (Kutner and Ulich 1981). This procedure yields a temperature scale T_A^* corrected for atmospheric attenuation, resistive losses, and rearward spillover and scattering. To correct for forward spillover and scattering, i.e., to derive intensities as independent as possible of the parameters of the telescope, T_A^* is divided by the main beam efficiency, η, the fraction of the forward power that enters the main beam, to yield the radiation temperature $T_R = T_A^*/\eta$, the physical temperature of a blackbody that just fills the main beam. Using the theoretical radiation pattern of the feed horn and the measured antenna pattern, as described in Appendix A, we derived $\eta = 0.82$ for the Chile Telescope, a value checked astronomically by observing the symmetrical CO shell around IRC +10216.

The survey spectra were taken to a noise level $\Delta T_A^* = 0.1$ K rms, each in typically 10 minutes of integration. Only linear baselines were subtracted. Standard CO calibration sources were observed daily with extremely repeatable results; the variation in the integrated antenna temperature of Orion A, for example, was only about 3% rms throughout the observation period. Pointing was checked daily by radiocontinuum observations of the Sun and every few months by observing stars with a small telescope collimated with the radio beam. The maximum pointing uncertainty was 1′, about 10% of the beamwidth.

Owing to small changes in the feed horn and secondary of

the Chile Telescope, its intensity scale disagrees slightly with that of the New York Telescope (in its several configurations). To compare the CO distribution in the fourth Galactic quadrant with that in the first, we need to calibrate the Southern temperature scale accurately against that of the Northern Survey. To transform the CO observations into H_2 column densities, both the Northern and Southern scales must be compared with that of the independent Northern Wide-Latitude CO Survey, or Wide Survey (Dame and Thaddeus 1985), which was made with the New York Telescope in a slightly different configuration from that used for the Northern Survey. The Wide Survey data, together with γ-ray data and H I 21 cm observations, were used by Bloemen *et al.* (1986) to derive the proportionality factor $X = 2.8 \times 10^{20}$ cm^{-2}(K km s^{-1})$^{-1}$ used here to convert CO luminosities, $W(\mathrm{CO}) = \int T(\mathrm{CO})dv$, to H_2 column densities, $N(H_2)$, hence to obtain H_2 masses.

By observing 16 positions in the Galactic plane and strong, well-defined sources like Orion A, our scale was determined to be 29% higher than that of the Northern Survey and 22% higher than that of the Wide Survey (Appendix A). About 13% is accounted for by an improved atmospheric model in the Southern calibration, leaving residual discrepancies of 14% and 8%, respectively—of order expected from minor instrumental differences and from an improved understanding of the antenna pattern.

The calibration of the Chile Telescope is probably the best determined of all three under consideration. However, for consistency, *we chose to adopt the scale of the Wide Survey as a standard* in order to use directly what we believe is so far the best CO-to-H_2 mass calibration. To put this choice into practice, the Northern radiation temperatures were multiplied by 1.06 (= 1.29/1.22) and the Southern ones divided by 1.22.

The H_2 masses obtained from our analysis are invariant to this choice of scale. If, for instance, we were to adopt the Chile Telescope as a standard, the CO emissivities would increase by 22%, but the X factor would decrease by the same factor, from 2.8 to 2.3 $\times$ 10^{20} cm^{-2}(K km s^{-1})$^{-1}$, leaving the H_2 column densities unchanged.

The H_2 masses given here are independent of the beam efficiencies and their attendant uncertainties; the X factor we use directly relates the H_2 column densities to the Northern Wide-Latitude CO Survey data, so only the calibration relative to that survey, which has been accurately obtained from astronomical observations, is needed.

For purposes other than deriving H_2 masses, temperatures here should be multiplied by 1.22 to obtain radiation temperatures in the Chile Telescope scale, T_R(Ch).

III. OBSERVATIONS

The Southern Deep CO Survey of the Milky Way (Table 1) comprises a total of ~7000 spectra spaced every beamwidth from $b = -0.^\circ75$ to $0.^\circ75$ (Fig. 1) and every two beamwidths beyond. The fully sampled region is 3 times as wide as in the Northern Survey, and the total latitude coverage is twice as wide. Each spectrum was integrated typically for 10 minutes, for a total observing time of 1400 hr. The sensitive receiver of the Chile Telescope, its excellent site, and the high transit of the fourth quadrant allowed the instrumental noise to be reduced to a low level: $\Delta T_R = 0.13$ K rms at a resolution of 1.3 km s^{-1}, about 4 times lower than that of the Northern Survey. The bandwidth of the spectrometer, 333 km s^{-1}, double that of the New York Telescope, was adequate to cover all velocities permitted by Galactic rotation, with many channels beyond to fit

TABLE 1

COLUMBIA SOUTHERN SURVEY

Parameter	Value
Galactic longitude	300°–348°
Galactic latitude	−2° to 2°
Radial velocity	300° ≤ l ≤ 335°: −166 to 166 km s^{-1} 335° < l ≤ 345°: −180 to 153 km s^{-1} 345° < l ≤ 348°: −218 to 114 km s^{-1}
Angular resolution	$0.^\circ147$
Sampling interval	$0.^\circ0 \le \lvert b \rvert \le 0.^\circ75$: $0.^\circ125$ $0.^\circ75 < \lvert b \rvert \le 2.^\circ0$: $0.^\circ25$
Sensitivity	$\Delta T_R = 0.13$ K rms at $\Delta t = 1.3$ km s^{-1}

baselines; the quality of the data can be judged from the sample spectra shown in Figures 4 and 5.

Position switching was used for all the observations; a set of 42 reference positions (Table 2), typically 2°–7° off the Galactic equator and less than 2° apart in longitude, selected in obscuration-free regions of the ESO plates, were shown by observation to be free of CO emission. Reference positions with lines stronger than 0.03 K (about one-third of the noise level of the survey spectra) were rejected.

To summarize the Southern Survey concisely in a two-dimensional map, the CO spectra were numerically integrated over the entire latitude coverage to obtain a standard longitude-velocity diagram (Fig. 6). As in the first quadrant (Dame *et al.* 1986), it is evident from the large-scale clumpiness of the emission that the molecular gas is organized into clouds

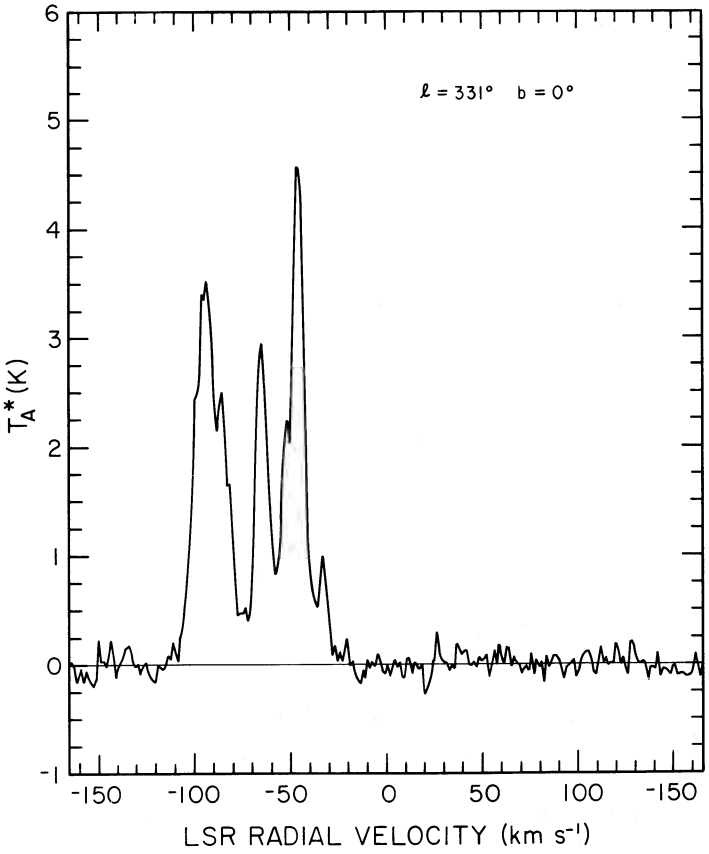

FIG. 4.—Typical CO spectrum from the Southern Survey

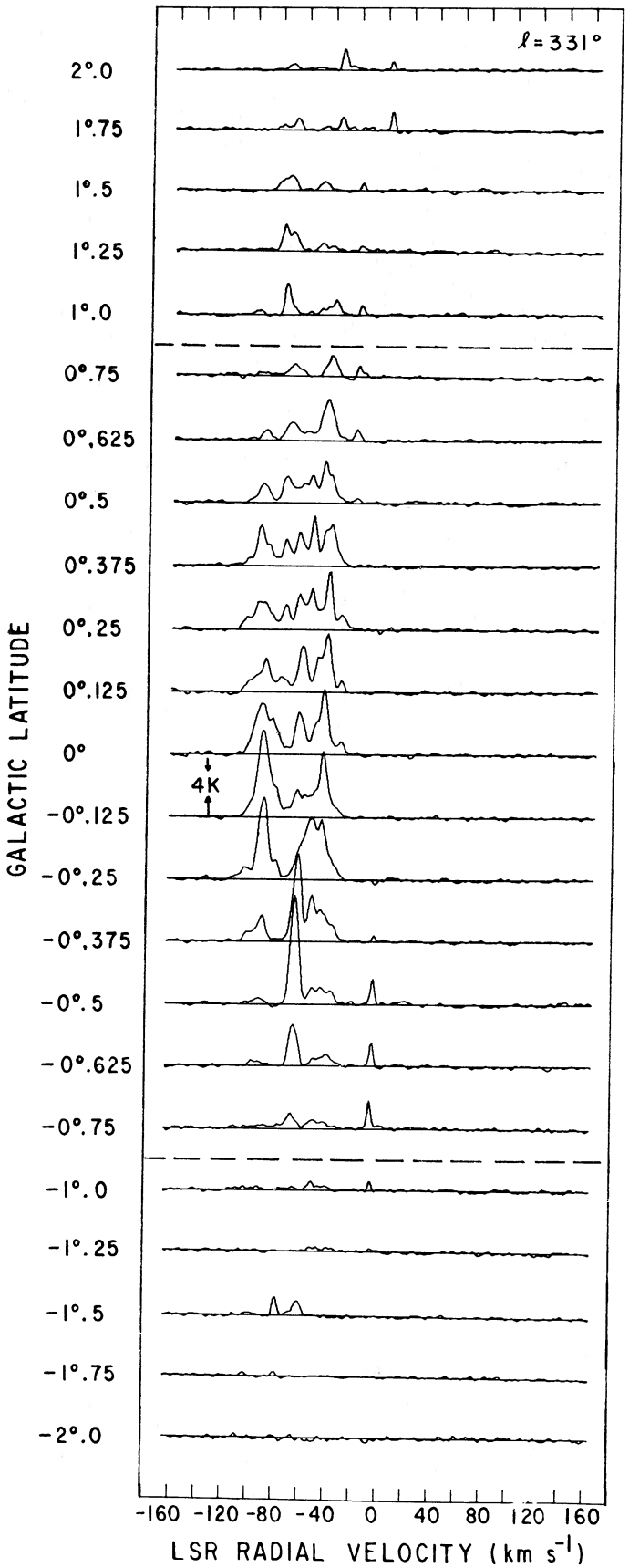

FIG. 5.—Sample spectra. The line of sight at $l = 331°$ apparently crosses several interior arms of the Galaxy, yielding the wide CO profiles observed. Dashed lines indicate the boundaries of the fully sampled regions.

TABLE 2

EMISSION-FREE REFERENCE POSITIONS

Longitude	Latitude
301.0	5.0
302.0	5.0
302.0	4.0
303.3	3.3
302.7	−2.7
306.8	−1.3
308.5	−3.2
311.0	−5.0
312.9	−3.4
316.0	−5.0
318.0	5.0
320.0	−3.6
323.0	−5.0
324.0	5.0
325.1	−6.2
326.0	3.0
326.0	5.0
327.0	5.0
328.1	−3.9
328.8	−1.8
330.0	8.0
330.5	4.0
331.0	−2.0
331.0	−7.0
332.0	−4.0
332.5	−2.0
333.0	8.0
334.0	2.0
334.0	−4.0
337.5	−6.8
338.5	7.7
339.0	5.0
339.0	5.0
340.0	2.0
342.7	−6.0
342.9	3.7
344.0	−5.0
344.3	5.8
346.0	−3.0
347.0	3.0
348.0	−5.0
353.0	4.0

and cloud complexes, but the distribution of the clouds differs significantly in the two hemispheres: the most intense emission in the south comes from the roughly triangular area ABC in the l, v diagram, which (assuming purely circular rotation) corresponds to a ring broader than that observed in the first quadrant, with a peak in intensity farther from the Galactic center (Cohen, Thaddeus, and Bronfman 1985).

A striking difference between the l, v diagrams of the Southern and Northern Surveys is the almost complete absence from the fourth quadrant of the Local arm (Dame *et al.* 1986), the prominent lane of CO clouds lying near zero velocity in the first quadrant. The most conspicuous local features in the Southern Survey are the Lupus clouds, between 341° and 348°, and the Coalsack, between 301° and 306°, both at velocities near zero. Farther from the Sun, but conspicuous over a wide distance range from ~2 kpc to more than 10 kpc, is the Carina spiral arm, its far side clearly traced by the clouds at 30 km s^{-1}, between 300° and 330°. Cohen *et al.* (1985) show that the molecular clouds in this arm and in the Sagittarius arm in the first quadrant apparently constitute a single, large-scale spiral feature extending over more than two-thirds of the way around the Galaxy.

The distribution of molecular complexes in the region of the

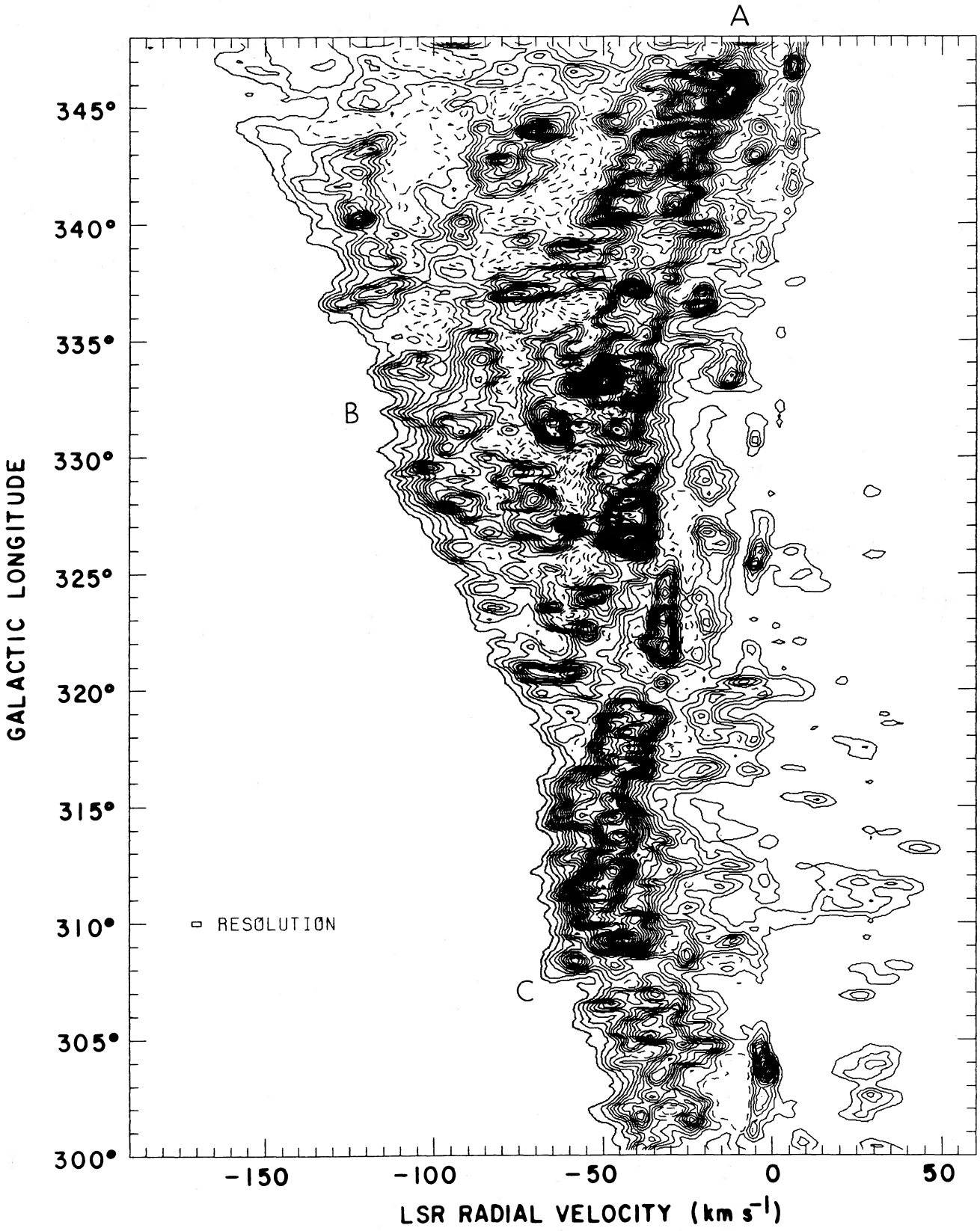

FIG. 6.—Longitude-velocity diagram obtained by integrating the Columbia CO Survey of the fourth Galactic quadrant across the Galactic plane. Contours denote equal values of $\int T_R\, db$ (§ II); the survey was integrated over $\pm 2°$ in latitude, and the contour interval is 0.4 K deg. The resolution is $0.°25 \times 2.6\,\mathrm{km\,s^{-1}}$.

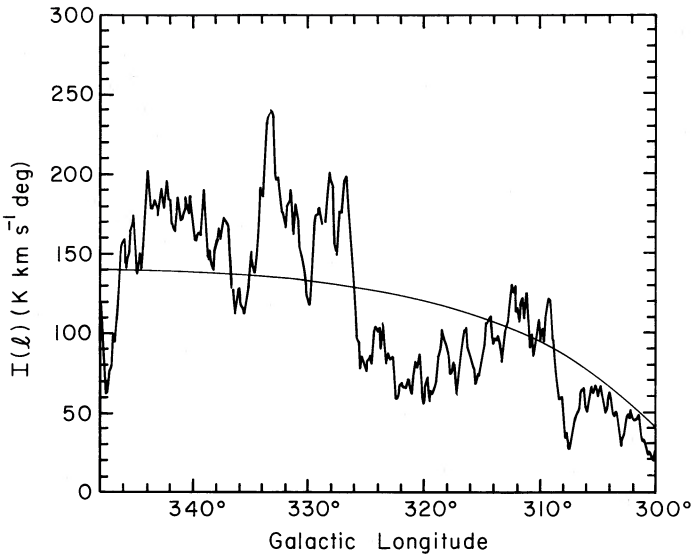

FIG. 7.—Longitudinal distribution of doubly integrated CO intensity $I(l) = \int T_R dV db$ in the southern Galaxy. The steps at $l = 310°$ and $l = 328°$ may mark the tangent points of the Centaurus and Norma spiral arms, respectively. The $I(l)$ predicted by our best-fit axisymmetric model is indicated by the smooth line.

Southern l, v diagram corresponding to the inner Galaxy is similar to that of H II regions (Courtès *et al.* 1970; Georgelin and Georgelin 1976) from which spiral arms have been derived. One such arm is apparently tangent to the line of sight at $l = 328°$, the Norma arm at roughly 8 kpc from the Galactic center, and another at 310°, the Centaurus arm at roughly 5 kpc. In a very tentative picture, the near side of the Centaurus arm (which may be the continuation in the fourth quadrant of the Scutum arm in the first) is traced by the complexes at 333°, -50 km s^{-1} and 327°, -45 km s^{-1} and by the lane of strong emission parallel to the longitude axis, from 310° to 320°, centered at -50 km s^{-1}; the near side of the Norma arm is traced by the complexes at 344°, -65 km s^{-1} and 328° to 335°, -100 to -80 km s^{-1}, a group that includes some of the most massive molecular clouds in the Galaxy (Bronfman *et al.* 1985). The region between 335° and 348°, from -100 to -150 km s^{-1}, is dominated by the 3 kpc expanding arm.

The longitudinal distribution of doubly integrated CO intensity, $I(l)$, is obtained by integrating in velocity the l, v diagram (Fig. 7). The steps in $I(l)$ at 310° and 328°, which roughly correspond to the lines of sight tangent to the Centaurus and Norma spiral arms, are among the best evidence for the existence of CO spiral arms in the inner Galaxy. Since the separation of the spiral arms is apparently wider in the fourth quadrant, the intensity contrast between different longitudes in the $I(l)$ graph is larger than for the northern distribution (Fig. 8).

The large amount of information in the Southern Survey concerning the spiral structure of the Galaxy requires a separate discussion and is deferred to a later paper. Here we perform only the simple but important axisymmetric analysis, in the attempt to find the general radial distribution of the molecular gas, the total H_2 mass, and the ratio of H_2 to H I for $R = 2$–10 kpc, the assumed radius of the solar circle.

IV. ANALYSIS

a) The CO-*to*-H_2 *Ratio*

The derivation of molecular cloud mass from our survey data is based on the widely made assumption that the velocity-integrated CO intensity, $W(CO)$, is directly proportional to the total H_2 column density in molecular clouds, $N(H_2)$, and is therefore proportional (with a correction of 1.38 to account for helium and heavier elements) to the total mass column density if the conversion of H into H_2 is complete.

No theoretical explanation yet given for this assumption is entirely adequate, because the small-scale structure and the details of radiative transfer in molecular clouds are largely unknown and undoubtedly complex. Its justification is essen-

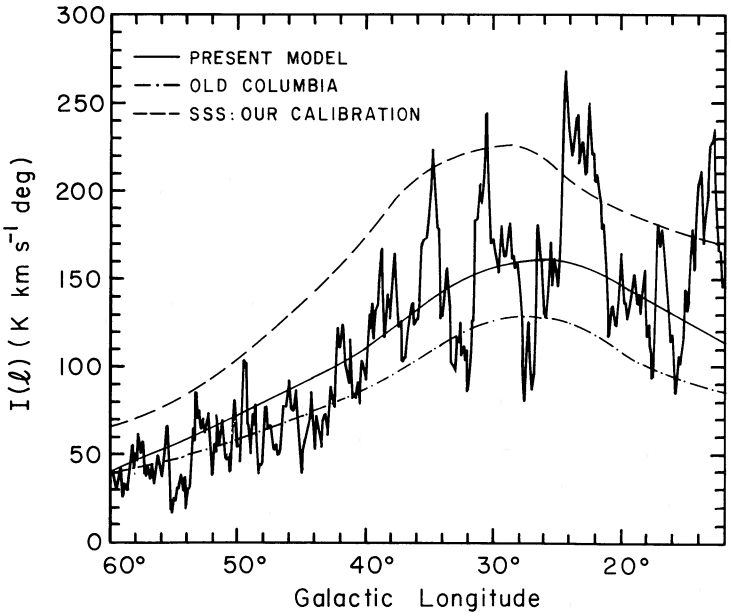

FIG. 8.—Longitudinal distribution of doubly integrated CO intensity in the northern Galaxy, compared with that predicted by our best-fit axisymmetric model, that from SSS analysis scaled down by a factor 1.20 to account for the different instrumental calibrations, and that from the previous Columbia analysis. The integral under the distribution predicted by our model is equal to that under the data to 1%.

tially empirical: the observational finding that the line profiles of normal CO not only are similar but also, when averaged over an appreciable fraction of most clouds, *are directly proportional* to the profiles of its rare isotopic species (i.e., ^{13}CO and $C^{18}O$), which are far less saturated and are generally thought to be the best available tracers of mass in molecular clouds. The velocity-integrated CO intensity, $W(CO)$, is apparently a measure of the column density of molecular clouds, $N(H_2)$, in roughly the same way that the luminosity of a globular cluster is a measure of its mass: by being proportional to the number column density of unresolved small objects that do not seriously overlap (with the advantageous difference that for the clumps within a molecular cloud occultation occurs only when overlap exists in both space and radial velocity).

Evidence on a Galactic scale in support of our fundamental assumption is the proportionality between the intensity of diffuse Galactic γ-rays (to which the interstellar medium is highly transparent) and a linear combination of CO luminosity and H I column density (Lebrun *et al.* 1983). By measuring the constant of proportionality, Bloemen *et al.* (1986) found the ratio of H_2 to CO to be

$$N(H_2)/W(CO) \equiv n(H_2)/\epsilon(CO) \equiv X = (2.8 \pm 0.4) \times 10^{20} \text{ cm}^{-2}(\text{K km s}^{-1})^{-1}, \quad (1)$$

where $N(H_2)$ and $n(H_2)$ are the usual column and number densities and $\epsilon(CO) \equiv dW_{CO}/ds$ (K km s^{-1} kpc^{-1}, where s is the distance along the line of sight) is defined as the CO volume emissivity. For consistency with previous work, no correction for helium has been made here in the conversion of CO intensities to H_2 densities.

b) *Axisymmetric Galactic Model*

Our goal is to determine the distribution of molecular gas as a function of distance from the Galactic center, R, and from the Galactic plane, z, without reference to the structure or mass spectrum of molecular clouds themselves. In other words, we will derive the smeared-out, average characteristics of the molecular gas on a scale of half a kiloparsec or more—much larger than the largest clouds observed. The clumpy structure of the clouds, however, cannot be neglected entirely; it must be taken into account in the statistical comparison of our smooth model and the observed gas distribution.

In our model, purely circular motion and axial symmetry of the gas distribution are assumed. The assumption of axial symmetry as a first approximation allows us to circumvent one of the main difficulties encountered by radio astronomers attempting to derive the structure of the inner Galaxy without distance measurements: the existence along the line of sight of two locations, "near" and "far," with the same radial velocity, i.e., the familiar twofold distance ambiguity. The technique used here is to derive an array of spectra from an axisymmetric model of the CO emissivity, ϵ (K km s^{-1} kpc^{-1}) (Burton *et al.* 1975; Cohen and Thaddeus 1977; Sanders, Solomon, and Scoville 1984), using a standard rotation curve (Burton and Gordon 1978). The parameters of the model are then adjusted through a maximum likelihood analysis to yield a best fit of the modeled spectra to the observed. The CO emissivity is assumed to be a Gaussian function of z with amplitude ϵ_0, displacement from the conventional Galactic plane z_0, and half-width $z_{1/2}$, all functions of R:

$$\epsilon(R, z) = \epsilon_0(R) \exp\{-[z - z_0(R)]^2[\ln 2]/[z_{1/2}(R)]^2\}. \quad (2)$$

To characterize the three functions $\epsilon_0(R)$, $z_0(R)$, and $z_{1/2}(R)$ with adequate radial resolution, yet without an excessive number of free parameters, the Galaxy is divided into concentric rings of thickness $\Delta R = 0.5$ kpc, each with constant ϵ_0, z_0, and $z_{1/2}$, for a total of 48 parameters between $R = 2$ kpc and 10 kpc. Since the velocity interval corresponding to a ring is wider than the largest line widths observed, the resultant correlation between rings can be ignored without significant error. As a consequence, the three parameters that characterize a given ring can be varied independently of those of other rings to fit only a small subset of the data. Thus, the seemingly formidable problem of determining 48 free parameters factors into a comparatively simple set of three-parameter fits, and issues of convergence and uniqueness, which can be extremely troublesome for fits with many degrees of freedom, are inconsequential.

In fitting the smooth theoretical model to the observed spectra, the clumpiness of the cloud distribution must be taken into account (Appendix B), because statistical fluctuations in the number of clouds are the main contribution to the variance in the distribution of line intensities, dominating instrumental noise. The assignment of weights and the differences between present and previous statistical analyses are discussed fully in Appendices B and C.

c) *The Molecular Galaxy*

Two data sets, symmetric with respect to the Galactic center, each 48° long ($l = 12°$–$60°$ and $l = 300°$–$348°$) and 2° wide ($b = -1°$ to 1°), were used to derive the radial distribution of molecular clouds between $R = 2$ kpc and 10 kpc. The results of the axisymmetric model applied to the first quadrant data (northern distribution), fourth quadrant (southern distribution), and combined data are shown in Figure 9 and Table 3. The shape of the distribution derived from the Northern data is in good agreement with previous results. The thickness of the molecular layer and its displacement from the conventional Galactic plane are essentially the same as those derived first by Cohen and Thaddeus (1977) and confirmed by SSS. The CO emissivity displays the characteristic sharply peaked "molecular ring," although, as shown in Figure 10 (and discussed in § V), in scale it differs significantly from previous work.

The molecular ring derived from the Southern data alone is considerably flatter and broader than that derived from the Northern data alone. The mean half-width at half-maximum of the molecular layer, 70 pc, is nearly the same in both hemispheres. The whole disk is gently warped in azimuth, the mean difference from north to south being about 17 pc, i.e., 24% of the half-width; the molecular layer is apparently inclined slightly with respect to the IAU plane. The well-known warp of the disk toward positive latitudes in the north and toward negative latitudes in the south, beyond the solar circle, is already apparent at $R \approx 9.75$ kpc; the displacement of the CO layer at that radius is 52 pc in the north and -74 pc in the south.

The axisymmetric model fit to the combined Northern and Southern data yields a ring with an inner radius of about 4 kpc and an outer radius of about 8 kpc, roughly flat between 4.5 kpc and 7.5 kpc. Owing to the azimuthal warping, the fit yields a molecular disk slightly thicker (75 pc HWHM) than the fit to either the Northern or the Southern data alone, with the emissivities somewhat lower than the average between north and south; however, as we shall see, the H_2 surface

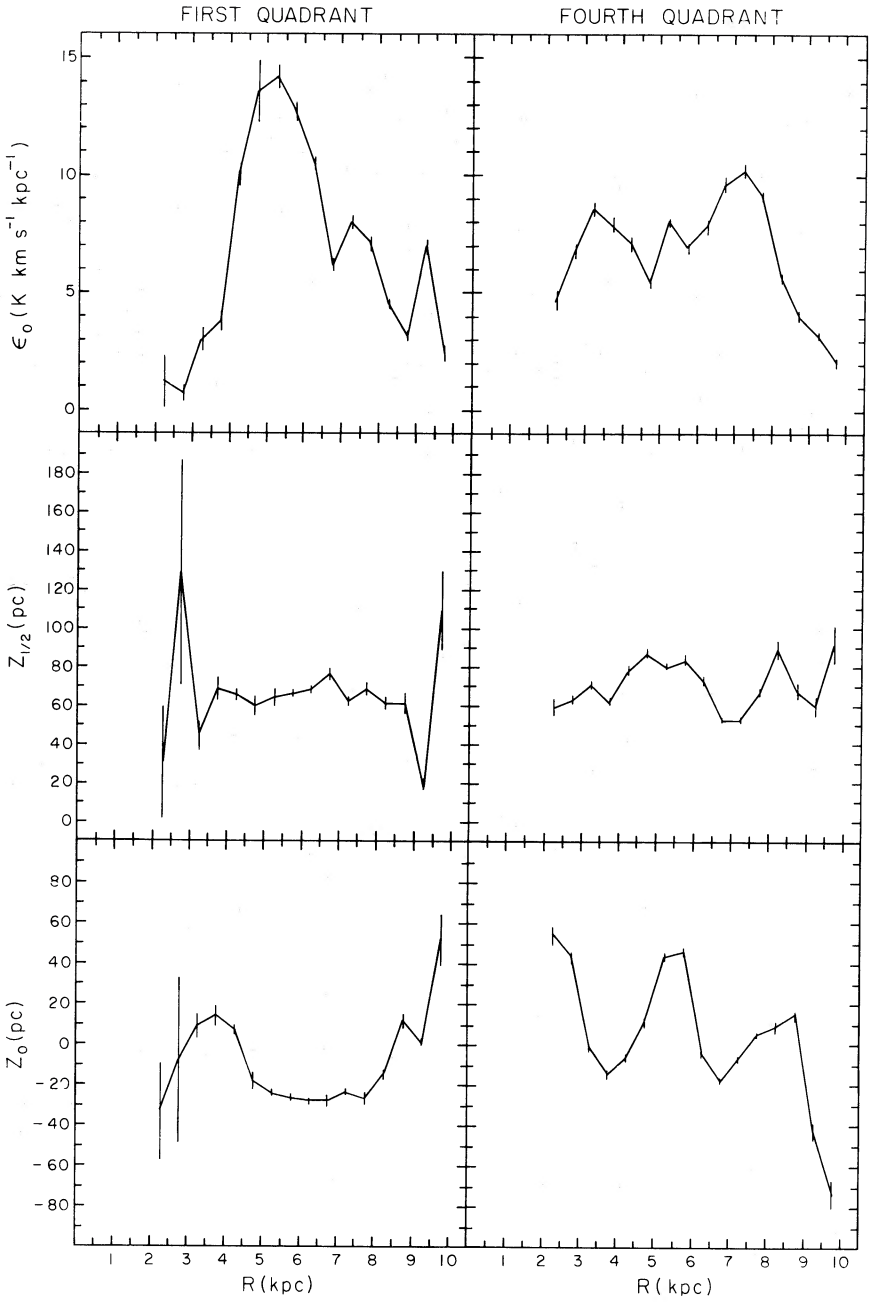

FIG. 9*a*

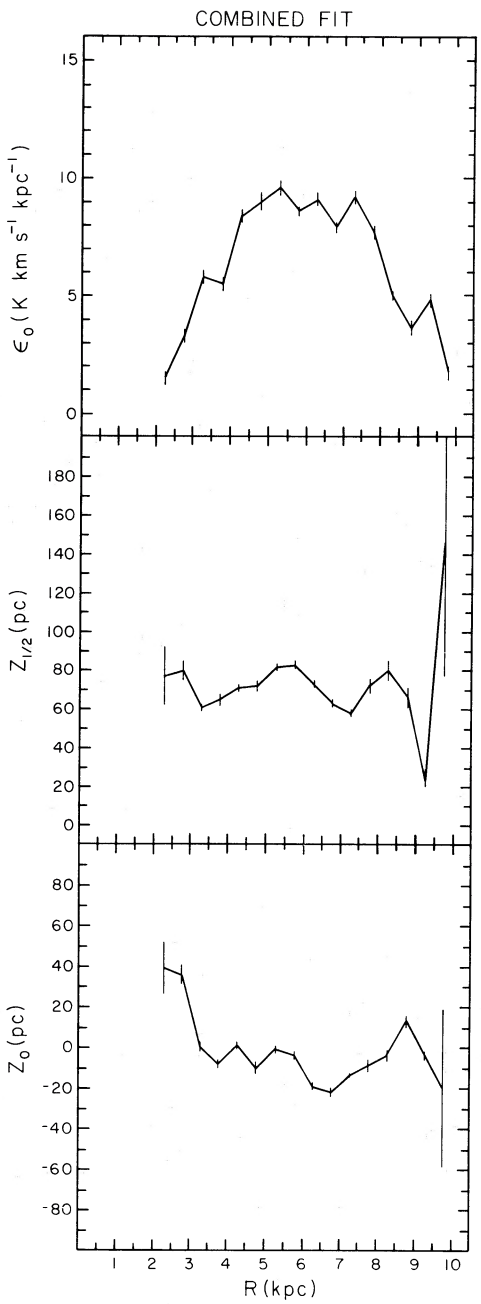

FIG. 9*b*

FIG. 9.—(*a*) Axisymmetric model of the CO distribution for $R = 2$–10 kpc, for the first and fourth quadrant data separately. Error bars represent the formal errors of the fit (1 σ) multiplied by a factor 6–10 to correct for the spatial and velocity correlation of the data within a typical molecular cloud (Appendix B). (*b*) Axisymmetric model of the CO distribution for $R = 2$–10 kpc, fitted to the combined Northern and Southern Surveys data.

density derived from the combined fit is nearly equal to that obtained from averaging the northern and southern distributions.

To test the self-consistency of our analysis, we compared the observed longitudinal distributions of doubly-integrated CO intensity $I(l) \equiv \int T(l, b, v)dvdb$, in the northern and southern hemispheres (Figs. 7 and 8), to those predicted from the model, $I^m(l) \equiv \int \epsilon\, dsdb$, and obtained an excellent agreement. In particular, when one averages over the entire longitude range of the survey, smearing out the fluctuations in $I(l)$, the observed triple integral, $I^{\text{total}} \equiv \int I(l)dl$, in both the north and south is reproduced to 1%.

The H_2 face-on surface density and the H_2 mass for $R = 2$–10 kpc are derived by integrating the number density of H_2 across the Galactic plane:

$$\sigma(R) = 2m_{\text{H}} \int_{-\infty}^{\infty} n(\text{H}_2)dz,$$

which for the assumed Gaussian distribution in z yields

$$\sigma(R) = (4\pi/\ln 2)^{1/2} X m_{\text{H}} \epsilon_0(R) z_{1/2}(R)\,, \qquad (3)$$

where m_{H} is the mass of atomic H. Although $\sigma(R)$ differs significantly in the first and fourth quadrants, (Fig. 11 and Table 4),

TABLE 3

BEST-FIT AXISYMMETRIC MODEL

R (kpc)	ϵ_0(N) (K km s^{-1})	ϵ_0(S) (K km s^{-1})	ϵ_0(C) (K km s^{-1})	z_0(N) (pc)	z_0(S) (pc)	z_0(C) (pc)	$z_{1/2}$(N) (pc)	$z_{1/2}$(S) (pc)	$z_{1/2}$(C) (pc)
2.25	1.2 ± 2.1	4.7 ± 0.8	1.5 ± 0.4	−33 ± 48	54 ± 8	39 ± 26	30 ± 59	59 ± 9	77 ± 30
2.75	0.7 ± 0.5	6.8 ± 0.6	3.3 ± 0.5	−8 ± 81	43 ± 5	36 ± 9	128 ± 117	63 ± 5	80 ± 10
3.25	3.0 ± 0.9	8.6 ± 0.6	5.8 ± 0.5	9 ± 12	−2 ± 4	0 ± 4	44 ± 13	70 ± 4	61 ± 4
3.75	3.8 ± 0.6	7.9 ± 0.6	5.5 ± 0.5	14 ± 10	−16 ± 4	−8 ± 4	68 ± 11	62 ± 4	65 ± 5
4.25	10.0 ± 0.9	7.1 ± 0.5	8.4 ± 0.5	7 ± 4	−7 ± 4	1 ± 3	65 ± 5	78 ± 5	71 ± 3
4.75	13.6 ± 2.5	5.4 ± 0.4	9.0 ± 0.8	−18 ± 8	11 ± 5	−10 ± 5	60 ± 9	87 ± 6	72 ± 5
5.25	14.2 ± 1.0	8.0 ± 0.4	9.6 ± 0.6	−24 ± 4	43 ± 4	−1 ± 4	66 ± 4	80 ± 5	82 ± 4
5.75	12.7 ± 0.8	6.9 ± 0.4	8.6 ± 0.4	−26 ± 3	46 ± 4	−4 ± 3	66 ± 4	83 ± 5	83 ± 4
6.25	10.5 ± 0.6	7.8 ± 0.5	9.1 ± 0.5	−28 ± 3	−5 ± 4	−19 ± 3	68 ± 4	73 ± 5	73 ± 3
6.75	6.1 ± 0.4	9.6 ± 0.6	7.9 ± 0.4	−28 ± 5	−18 ± 3	−22 ± 3	76 ± 7	53 ± 3	63 ± 4
7.25	8.0 ± 0.5	10.2 ± 0.6	9.2 ± 0.5	−24 ± 3	−8 ± 2	−14 ± 3	62 ± 4	53 ± 3	58 ± 4
7.75	7.1 ± 0.6	9.1 ± 0.4	7.7 ± 0.5	−27 ± 6	5 ± 3	−9 ± 5	68 ± 7	66 ± 4	72 ± 7
8.25	4.5 ± 0.3	5.6 ± 0.3	5.0 ± 0.3	−15 ± 4	8 ± 5	−4 ± 5	61 ± 6	89 ± 10	80 ± 9
8.75	3.1 ± 0.3	4.0 ± 0.2	3.6 ± 0.6	12 ± 6	14 ± 4	13 ± 6	61 ± 10	67 ± 7	66 ± 10
9.25	7.0 ± 0.6	3.1 ± 0.3	4.8 ± 0.6	0 ± 1	−43 ± 8	−4 ± 3	18 ± 3	59 ± 10	23 ± 5
9.75	2.4 ± 0.5	2.0 ± 0.3	1.7 ± 0.5	52 ± 25	−74 ± 14	−20 ± 77	109 ± 40	92 ± 18	147 ± 139

NOTE.—N = northern distribution, S = southern distribution, C = combined distribution.

the total H_2 mass, $M(H_2) \approx 1.2 \times 10^9\ M_\odot$, and the mean radius, $\langle R \rangle \approx 6.5$ kpc, are remarkably similar north and south (Table 5). The peaks at 5 kpc in the north and at 8 kpc in the south correspond to a classical spiral arm (e.g., Georgelin and Georgelin 1976; Dame 1983), namely the Scutum-Centaurus arm, tangent to the line of sight at $l = 30°$ and 310°, which opens toward the solar circle in the fourth quadrant. The arm may be partly responsible for the enhancement of the H_2 number density (Fig. 12 and Table 4) in these regions. The H_2 surface density radial distribution averaged over the first and fourth Galactic quadrants (Fig. 13), as expected from self-consistency, is roughly equal to that obtained from fitting the axisymmetric model to the combined Northern and Southern data.

For the southern hemisphere, the derivation included a correction for deviations from purely circular motion within 4 kpc of the Galactic center. The surface density, $\sigma(R)$, for R smaller than ~4 kpc, when derived directly from the axisymmetric model, is overestimated in the south and underestimated in the north, owing to the expanding 3 kpc arm (Rougoor and Oort 1960), which in the l, v diagram appears displaced toward negative velocities from the position it would have were the same molecular clouds only in circular motion. In the southern hemisphere, the expansion displaces the emission toward an

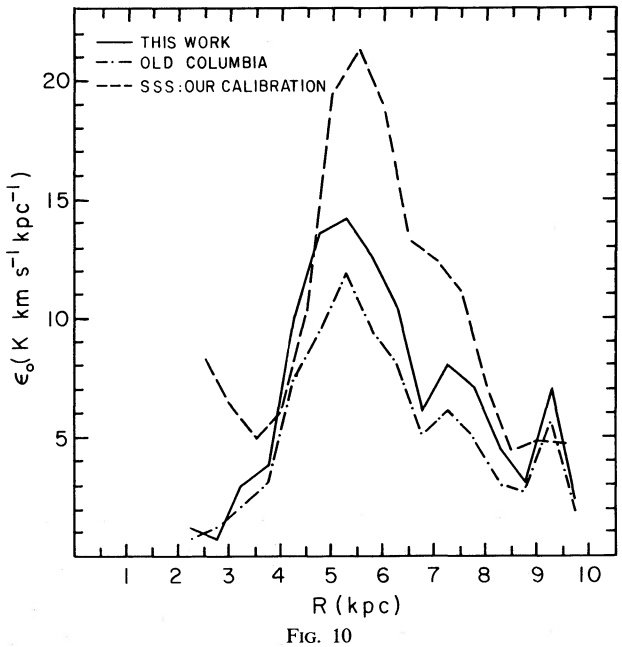

FIG. 10

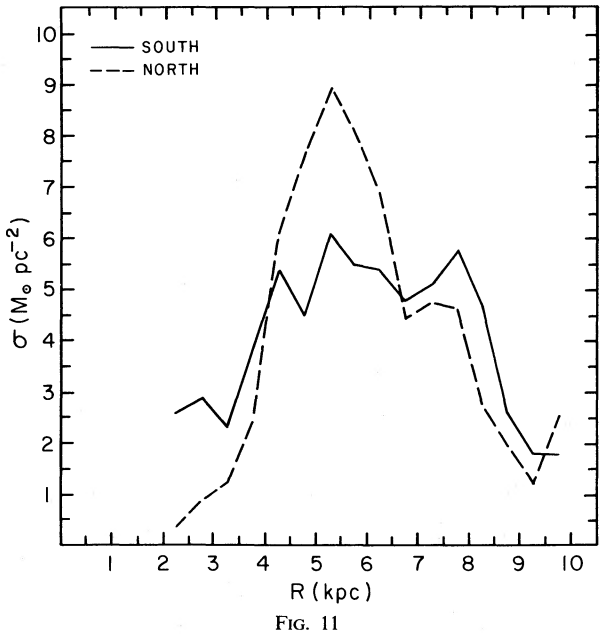

FIG. 11

FIG. 10.—The northern CO emissivity derived here, by SSS, and by the previous Columbia analysis, all in the same temperature scale (the one used here). The disagreement is due only to differences in the statistical analyses.

FIG. 11.—Galactic face-on surface-density of H_2 derived by fitting axisymmetric models to the Northern and Southern CO Surveys separately. As discussed in the text, there has been a small correction in the southern distribution for noncircular motion of the 3 kpc arm.

TABLE 4

H_2 SURFACE DENSITY AND IN-PLANE NUMBER DENSITY NORTH AND SOUTH

	NORTH		SOUTH	
R (kpc)	$\sigma(H_2)$ ($M_\odot$ pc^{-2})	$n_0(H_2)$ (cm^{-3})	$\sigma(H_2)$ ($M_\odot$ pc^{-2})	$n_0(H_2)$ (cm^{-3})
2.25	0.3	0.11	2.6	0.42
2.75	0.9	0.07	2.9	0.49
3.25	1.3	0.27	2.3	0.38
3.75	2.5	0.34	3.9	0.63
4.25	6.3	0.91	5.4	0.65
4.75	7.7	1.23	4.5	0.49
5.25	9.0	1.29	6.1	0.72
5.75	8.1	1.15	5.5	0.63
6.25	6.8	0.95	5.4	0.71
6.75	4.5	0.56	4.8	0.87
7.25	4.8	0.73	5.1	0.93
7.75	4.6	0.64	5.8	0.83
8.25	2.7	0.41	4.7	0.50
8.75	1.9	0.28	2.6	0.37
9.25	1.2	0.63	1.8	0.29
9.75	2.5	0.22	1.8	0.18

empty region of the l, v diagram, making the 3 kpc arm one of the more conspicuous features. To correct for this effect, the projection in the l, v diagram of a circular arm 1 kpc wide, located at $R = 4$ kpc, with a circular velocity given by the rotation curve, and expanding at 50 km s^{-1}, was removed from the Southern data set. The axisymmetric model was applied to this corrected data set, and the H_2 surface density recalculated. The contribution of the arm to the surface density was then computed separately, on the assumption that the arm, because seen in absorption against the Galactic center, is at the near distance (Fig. 14). A value of 10^7 $M_\odot$ was obtained for the H_2 mass of the arm between $l \approx 335°$ and 348°. The correction lowered by 4% the total H_2 mass obtained from the Southern data for $R = 2$–10 kpc.

Correction to the total mass for the 3 kpc arm is difficult to make in analyzing the Northern data, because for $l \geq 12°$ this arm is blended with strong emission from larger R. We estimate this correction to the total mass, not included in Figure 11 and Table 4, to be between 0 and −4%; it would affect only slightly the density distribution in Figure 11 between 4 kpc and 10 kpc.

A further check on self-consistency was made by exploiting the familiar "latitude effect," i.e., by adopting $z_0(R)$ and $z_{1/2}(R)$ from the best-fit model—quantities on which observers now generally agree—and then calculating $\epsilon_0(R)$ by partitioning the CO emission in a given direction and velocity between near and far distances with a weight that depended on the near or far distance from the plane, z. The weighting function $w(z)$ was simply the Guassian distribution assumed in our model,

$$w(z) \equiv A \exp\{-[z - z_0(R)]^2 \ln 2/[z_{1/2}(R)]^2\}, \quad (4)$$

where A is a normalization constant. The surface density of H_2 as a function of R obtained in this "direct way" (Fig. 15) is in excellent agreement with that obtained from the full model, the total mass being only 6% lower. The sensitivity of the total mass to the parameters was further tested by simplifying the calculation, using constant values of the parameters, $z_0 = 0$ pc and $z_{1/2} = 70$ pc; the mass changed by only 1%; varying $z_{1/2}$ in a range from 40 to 100 pc changed the mass by only 20%. The important conclusion to be drawn from these checks is that the molecular mass we derive between $R = 2$ kpc and 10 kpc is largely independent of the model, and that the pro-

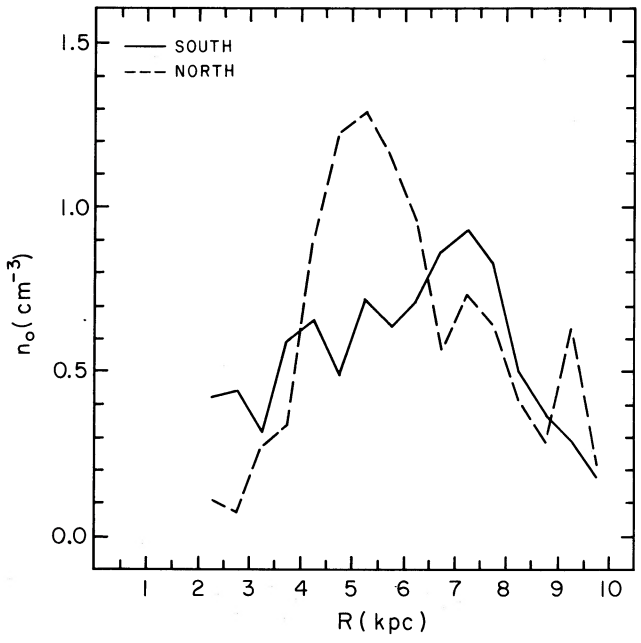

FIG. 12

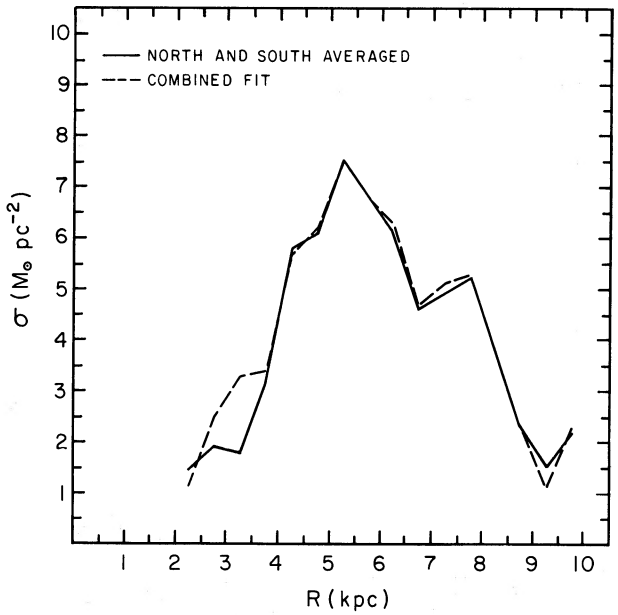

FIG. 13

FIG. 12.—Number density of H_2 at the centroid of the molecular layer derived by fitting axisymmetric models to the Northern and Southern CO Surveys separately.

FIG. 13.—Average of the northern and southern face-on surface densities of H_2 in Fig. 11, compared to that obtained by fitting an axisymmetric model to the combined Northern and Southern CO Surveys. The difference at $R < 4$ kpc arises from the correction for radial motions of the 4 kpc arm applied to the Southern CO Survey analysis.

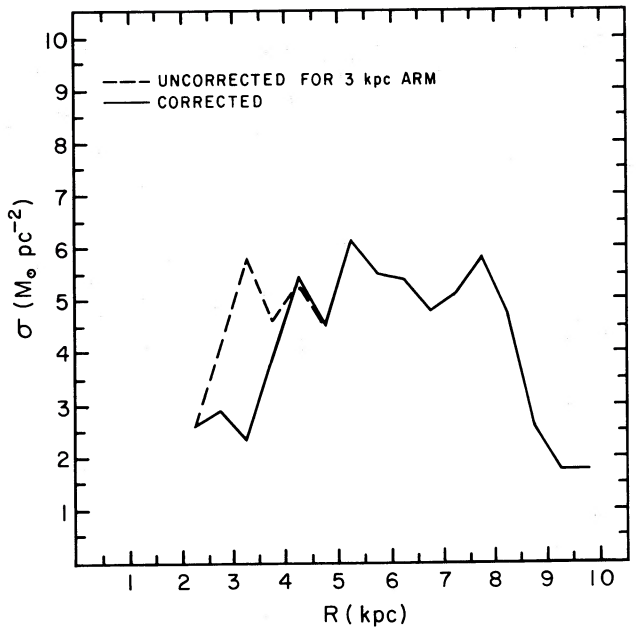

FIG. 14.—Galactic face-on surface-density of H_2 derived from the Southern CO Survey corrected for radial motions of the 4 kpc arms and uncorrected.

cedure employed to fit the model to our survey data is therefore realistic and self-consistent.

V. DISCUSSION

a) Molecular to Atomic Mass

Using $0.9 \times 10^9\ M_\odot$ (Henderson *et al.* 1982; Bloemen *et al.* 1986) for the H I mass, we obtained a global ratio $M(H_2)/M(\text{H I})$ of 1.3 for $R = 2$–10 kpc, in good agreement with the estimate of equipartition made by Cohen *et al.* (1980) and by Thaddeus and Dame (1984). Bloemen *et al.* (1986) obtained, from the Wide Survey, a value of 1.0, in satisfactory agreement, given the simplifying assumption made in their calculation, i.e., that the H I and H_2 densities are proportional.

A ratio $M(H_2)/M(\text{H I})$ for $R = 2$–10 kpc more than twice as large was derived by SSS using the Stony Brook/Massachusetts CO Survey data and an axisymmetric model similar to ours. Their survey, although undersampled by a factor of about 800 in solid angle, represents a coverage comparable to that of the Columbia Northern Survey; it comprises a total of 1300 spectra taken at resolutions of 45″ and 65″, in a region from $l = 4°$ to 70° and from $b = -2°$ to 2°. The axisymmetric analysis by SSS agrees qualitatively with ours here and that of Cohen and Thaddeus (1977). The thickness and displacement of the northern molecular disk are nearly the same as ours and the general radial shape of their CO distribution also is similar, but the H_2 surface density distribution they obtain differs from the one here in scale (Fig. 16): their value for the total H_2 mass between $R = 2$ kpc and 10 kpc is $2.7 \times 10^9\ M_\odot$, versus our $1.2 \times 10^9\ M_\odot$. Of the main sources of disagreement, two are simply scale factors: different instrumental calibrations and a different $N(H_2)$–to–$W(\text{CO})$ ratio. A third factor, not previously identified, arises from their use of a different method of statistical analysis.

We checked the spectral line calibration of SSS by comparing the observed velocity integrated emission, $W(\text{CO})$, for 25 positions at $b = 0°$, between $l = 12°$ and 60°, common to both surveys (Appendix A). For f_{cal}, the ratio of the averaged W_{CO}, we find

$$f_{\text{cal}} \equiv \langle W(\text{SSS})\rangle / \langle W(\text{this work})\rangle = 1.20 \pm 0.03\ , \qquad (5)$$

where the uncertainty results from instrumental noise.

The adopted X conversion factors are in the ratio

$$f_X \equiv X_{\text{SSS}}/X_{\text{this work}} = (3.6 \times 10^{20})/(2.8 \times 10^{20}) = 1.29\ . \qquad (6)$$

The value of X used by SSS is based on several uncertain factors, including the ratio of ^{13}CO to extinction,

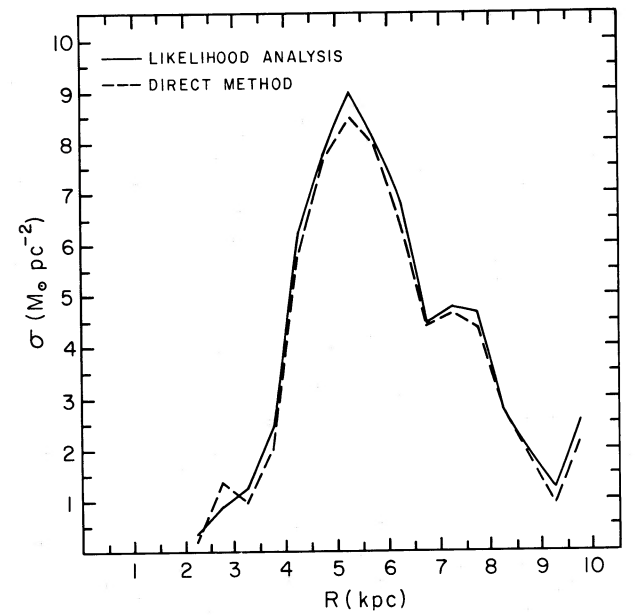

FIG. 15.—The northern H_2 surface-density distribution from the axisymmetric model compared to that calculated directly by partitioning the emission between "near" and "far" according to latitude, as described in § IV.

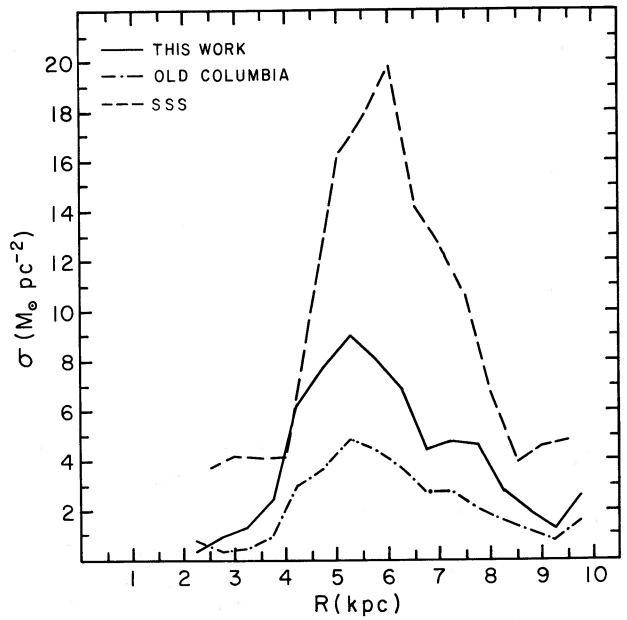

FIG. 16.—Comparison of the northern H_2 surface-density reported here with that derived by Sanders, Solomon, and Scoville (1984) and with the old Columbia results (Thaddeus and Dame 1984).

$\int T(^{13}\mathrm{CO})dv/A_v$, and the ratio of CO to ^{13}CO. The value of X used in the present work relies on a somewhat simpler chain of reasoning and agrees well with the latest determinations based on extinction measurements (Bloemen *et al.* 1986).

Although our X conversion factor would be ~20% smaller if Bloemen *et al.* had used the calibration of the Chile Telescope, the H_2 masses here, as already emphasized, would remain unchanged. Bloemen *et al.* assumed that the observed high-energy ($E > 300$ MeV) γ-ray flux from the Galactic plane results from the interaction of cosmic rays with the interstellar gas and also that the density of cosmic rays in the Galaxy is uniform, so that the γ-ray flux is directly proportional to the number of nucleons in the line of sight, i.e., $I(\gamma) = q[N(\mathrm{H\ I}) + 2XW(\mathrm{CO})]$, where $I(\gamma)$ is the measured γ-ray flux and N(H I) and W(CO) are the measured H I column density and CO luminosity. Two parameters were adjusted in their analysis: the conversion factor X and the γ-ray emissivity per nucleon q. A change in the CO temperature scale would not affect $N(H_2)$, because it would produce a compensating change in X and leave the product $f_{\mathrm{cal}}f_X$ unchanged. Similarly, scale changes in the γ-ray intensity or in the 21 cm line calibration would have modified the fitted parameters, without affecting the ratio $M(H_2)/M(\mathrm{H\ I})$. Thus, although $M(H_2)$ depends directly on M(H I), the ratio of the two is largely free of systematic uncertainties in the instrumental calibrations. As an illustration, note that a molecular cloud and an atomic cloud with the same γ-ray luminosity would be assigned equal masses regardless of their H I and CO luminosities—or calibrations.

The different calibrations and X factors do not completely resolve the disagreement in the H_2 mass between SSS and this work. Even when these are taken into account by scaling down the SSS H_2 surface density by $f_{\mathrm{cal}} \times f_X = 1.55$ (Fig. 17), their H_2 mass between 2 kpc and 10 kpc is still 42% larger than ours.

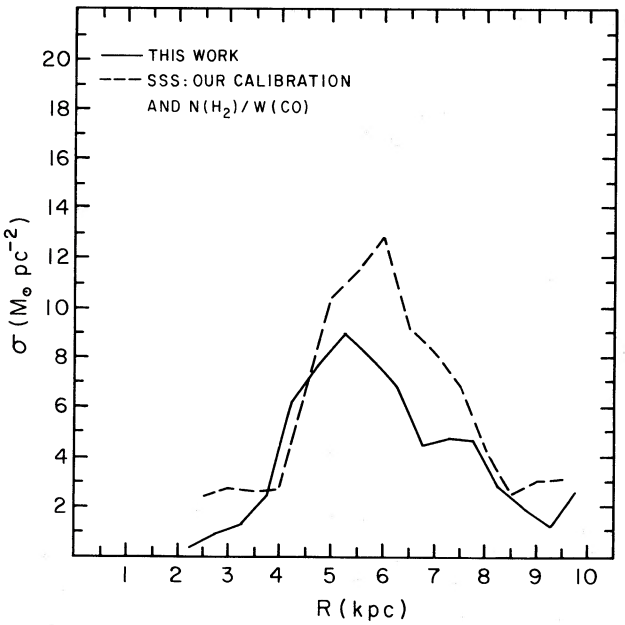

FIG. 17.—The northern H_2 surface-density distribution of Sanders, Solomon, and Scoville (1984), scaled down by a factor 1.55 to account for the differences in calibration and in $N(H_2)/W(\mathrm{CO})$, compared with that derived from the Columbia Northern CO Survey. The residual 40% discrepancy in the total H_2 mass between $R = 2$ kpc and 10 kpc is attributed to differences in assigning weights when fitting an axisymmetric model to the data.

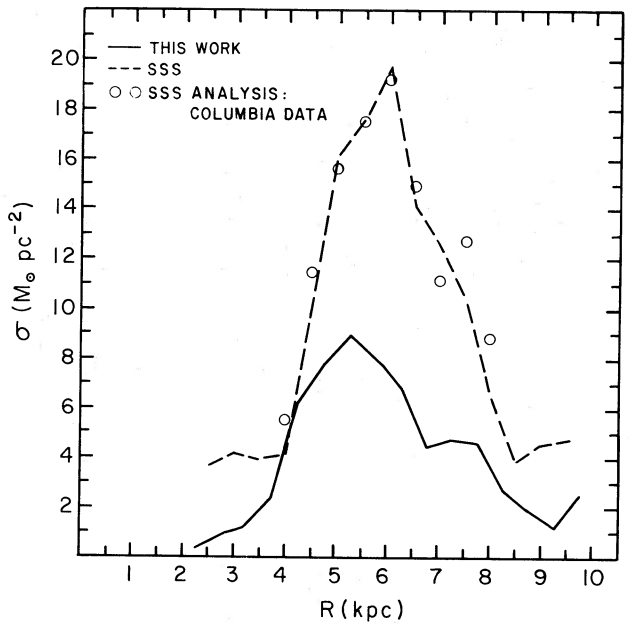

FIG. 18.—The northern H_2 surface-density distribution derived using Columbia data, and SSS calibration, $N(H_2)/W(\mathrm{CO})$ ratio, and analysis method compared to the SSS original results (*dashed line*). The results obtained using our analysis are also shown for reference.

To demonstrate that this residual discrepancy is the result of the different weights adopted in fitting the model to the data, we reanalyzed the Northern Survey, using the SSS calibration and X factor and following their method as closely as possible, and obtained essentially their results (Fig. 18). The resultant surface density, using our data, is only 5% higher than the original SSS value for $R = 4$–8 kpc, and at the peak of the molecular ring, for $R = 4.75$–6.75 kpc, is within 1%. Thus, we can now entirely account for the overall discrepancy in mass between SSS and this work. The ratio of the H_2 masses can be factored as

$$M(\mathrm{H_2})_{\mathrm{SSS}}/M(\mathrm{H_2})_{\mathrm{this\ work}} = f_{\mathrm{cal}}f_X f_{\mathrm{stat}} \approx 1.2 \times 1.3 \times 1.4\,. \quad (7)$$

Unlike ours, the axisymmetric analysis of SSS does not reproduce the longitudinal distribution of integrated CO intensity (Fig. 8) and therefore is not self-consistent. Their method predicts an integrated CO intensity averaged between 12° and 60° that is ~40% larger than that observed. For this reason and other arguments given in Appendices B and C, our analysis, we think, is the more realistic and yields a more accurate determination of the mean radial distribution of molecular gas in the Galaxy. Although the H_2 surface density may double that of H I when averaged over the northern molecular ring alone, the global ratio of $M(H_2)$ to M(H I) is of order unity for $R = 2$–10 kpc.

b) The Molecular Disk

The separate fits of the axisymmetric model to the first and fourth quadrant data yield results sufficiently different to suggest large-scale deviations from azimuthal symmetry. The flatter, broader radial distribution of molecular gas density in the southern Galaxy is readily understood if the radial distribution is an average over spiral arms that open up in the fourth Galactic quadrant (Kerr 1970; Weaver 1970; Georgelin

and Georgelin 1976). These results are in good qualitative agreement with those obtained by Robinson *et al.* (1984) from a comparison of their southern CO survey and the Stony Brook/Massachusetts CO Survey (SSS).

The CO emissivity radial distribution at $b = 0°$ obtained by Robinson *et al.* from their survey, a longitude strip going from 294° to 358°, at $b = 0°$, fully sampled at a resolution of 0°.15, is similar in shape to that obtained from our data. However, a scale difference of the order of the difference between the results of SSS and our Northern results arises from instrumental calibration and from the different methods used to determine the CO emissivity at $b = 0°$. This is hardly surprising, since the calibration of Robinson *et al.* was derived from the Stony Brook/Massachusetts Survey, and their method of analysis is that of SSS restricted to $b = 0°$ (Appendix C).

The nearly identical mean half-width of the CO layer, $\langle z_{1/2} \rangle$ (Table 5), in the first and fourth quadrants is both expected and gratifying. Because the thickness of the molecular disk is strongly dependent on the gravitational potential of the Galaxy, which presumably is quite axisymmetric because it results mainly from the distribution of old stars, a significant north-south difference in $\langle z_{1/2} \rangle$ would be surprising, and perhaps an indication of bias in the data or error in the analysis. It is also worth calling attention to the fact that $\langle R \rangle$, the mass weighted mean molecular radius between $R = 2$ kpc and 10 kpc, is nearly the same north and south, although the southern distribution, as we have seen, is much flatter in R than the northern.

Using the value of $M(H_2)$ derived here, and the molecular cloud mass spectrum given by Dame *et al.* (1986), with an upper cutoff at $5 \times 10^6\ M_\odot$, we predict for $R = 2$–10 kpc a total of ~500 clouds in the upper mass decade, i.e., between $5 \times 10^5\ M_\odot$ and $5 \times 10^6\ M_\odot$. The mean distance between these clouds is of order 700 pc, which is roughly the same as the mean distance between molecular cloud complexes in the Carina spiral arm (Grabelsky *et al.* 1987).

The H_2 surface density averaged between $R = 9$ kpc and 10 kpc derived in this work, 1.7 $M_\odot$ pc^{-2}, is in satisfactory agreement with the average H_2 surface density within 1 kpc of the Sun (Dame *et al.* 1987), 1.3 $M_\odot$ pc^{-2}, obtained by summing the masses of the largest observed molecular clouds. Beyond the solar circle, in the southern Galaxy, the H_2 surface density, averaged in rings 0.5 kpc wide over a longitude range from 280° to 335°, is 1.6 $M_\odot$ pc^{-2} at $R = 10.5$ kpc (Grabelsky *et al.* 1987), in good agreement with the value for $R = 9.75$ kpc in the fourth quadrant given in this work, 1.8 $M_\odot$ pc^{-2}.

TABLE 5

SEPARATE AXISYMMETRIC MODELS: $R = 2$–10 kpc

Parameter	North	South
Total molecular mass (M)	$1.21 \times 10^9\ M_\odot$	$1.20 \times 10^9\ M_\odot$
Average H_2 surface density	4.0 $M_\odot$ pc^{-2}	4.0 $M_\odot$ pc^{-2}
Mean radius $\langle R \rangle$	6.5 kpc	6.6 kpc
Mean half-width $\langle z_{1/2} \rangle$	68 pc	71 pc
Mean displacement $\langle z_0 \rangle$	−14 pc	3 pc

NOTE.—Mean quantities are mass weighted: $\langle X \rangle \equiv \sum X(R)\Delta M(R) / \sum \Delta M(R)$, where $X(R)$ is the value of X obtained from the axisymmetric model for the ring of radius R and width ΔR, and $\Delta M(R)$ is the molecular mass contained in such ring.

VI. SUMMARY

The first out-of-plane CO survey of the southern Milky Way has been completed with the Columbia Millimeter-Wave Telescope at Cerro Tololo, Chile. This Southern Survey, covering the area from $l = 300°$ to 348° within 2° of the plane, is a mirror image, with better sampling and coverage, of the Columbia Northern Survey. Together, these represent the first homogeneous and complete survey of molecular clouds in the inner Galaxy.

The distribution of molecular clouds differs significantly in the two hemispheres, that in the south being significantly flatter in R than that in the north. There is clear evidence for the existence of spiral arms in the fourth Galactic quadrant from the steps in the longitudinal distribution of doubly integrated CO intensity, $I(l)$, at $l = 310°$ and 328°, but all such azimuthally dependent features were averaged in the axisymmetric analysis undertaken here.

An axisymmetric model fit separately to the Northern and Southern data shows a molecular disk of roughly constant half-thickness, ~70 pc, with a smooth azimuthal warp, slightly inclined with respect to the conventional IAU plane. The density peak at 5 kpc in the north broadens in the south into a plateau, from 4 kpc to 8 kpc from the Galactic center. The total mass of H_2 between $R = 2$ kpc and 10 kpc separately derived from the Northern and Southern Surveys is nearly identical: $1.2 \times 10^9\ M_\odot$. The combined analysis of these Surveys shows that about 70% of the molecular gas lies in a ring 4 kpc wide with a mean radius of 6.5 kpc. The ratio of H_2 to H I, which is 2 for $R = 4$–8 kpc in the northern molecular ring, is 1.3 for $R = 2$–10 kpc. The present analysis is self-consistent in that it can reproduce the observed longitudinal distribution of integrated CO intensity, $I(l)$. In particular, the total integrated CO emission, $\int I(l)dl$, is reproduced to an accuracy of 1% for both surveys.

A similar axisymmetric analysis of an independent survey by Sanders, Solomon, and Scoville (1984) agrees qualitatively with ours here, but there are significant quantitative discrepancies. In particular, the total integrated CO emission, $\int I(l)dl$, predicted by their analysis is on average 40% higher than that observed, and their value for the total H_2 mass is 2.2 times larger than ours. This ratio has been resolved into three main factors, all tending to increase the difference between their H_2 mass and ours: different instrumental calibrations (20%), different ratios of H_2 to CO (i.e., $N(H_2)/W(CO)$ (30%), and differences in the statistical analysis (40%) of the data. To demonstrate that the last factor results from the different ways of deriving the axisymmetric Galaxy from the data sets, we analyzed our data in the way SSS analyzed theirs and obtained their results.

The confinement of molecular clouds to spiral arms, suggested both by the rough equipartition of atomic and molecular gas in the Galactic disk within the solar circle and by the azimuthal asymmetry of the molecular cloud distribution, stands out now as the most interesting subject for the next step in the joint analysis of the Columbia Northern and Southern Deep CO Surveys.

We thank T. M. Dame, D. A. Grabelsky, L.-Å. Nyman, and E. S. Palmer for helpful discussions, F. Avilés, M. Koprucu, and J. Montani for help with the operation and maintenance of the 1.2 m Southern Telescope, A. V. Smith for help with data

analysis, and E. Sarot for editorial assistance. The staff of the Cerro Tololo Inter-American Observatory provided valuable support during the period of observations.

We are indebted to C. Lacey, who emphasized the value of the doubly integrated CO emission as a self-consistency test, and to A. Strong, who suggested the alternative mass computation (§ IV). We are also grateful to an anonymous referee for several helpful comments.

This work was supported by a grant from the National Science Foundation.

L. B. acknowledges partial support by Fondo Nacional de Educación y Ciencias de la Republica de Chile.

APPENDIX A

INSTRUMENTAL CALIBRATION

I. MAIN BEAM EFFICIENCY

The main beam efficiency, η, is defined here as the fraction of the forward power that enters the main beam. Using the theoretical radiation pattern of the feed horn, we estimate that roughly 8% of the forward power is lost to spillover around the secondary and 1% is lost through a small central alignment hole in the secondary. Of the remaining 91% illuminating the secondary, using scalar diffraction theory and the measured antenna pattern (Bronfman 1986) we calculated that $\sim 2\%$ is scattered into far sidelobes, 8% into near sidelobes, and 90% enters the main beam. The main beam efficiency is therefore $\eta = 0.91 \times 0.90 = 0.82$. The diameter of our main beam to the first null, containing 82% of the forward power, is $\sim 23'$, and the diameter of the beam to the second null, containing 87% of the forward power, is $\sim 46'$.

The beam efficiency was checked astronomically by observing the symmetrical CO shell with a diameter of $\sim 140''$ around the evolved star IRC +10216 (Kwan and Hill 1977). The observed peak temperature at the center of the line was (0.42 ± 0.02) K, and the velocity-integrated temperature (9.26 ± 0.15) K km s^{-1}. The CO brightness temperature distribution of IRC +10216 has been modeled by Kwan and Linke (1982), who adjusted the parameters of their model to reproduce observations made with the Bell Telephone Laboratories (BTL) 7 m telescope and the Five College Radio Astronomy Observatory (FCRAO) 14 m telescope. Comparing the observed temperature of IRC +10216 to the radiation temperature predicted by convolving our beam with the model, we obtained a value of $\eta = 0.81 \pm 0.05$.

The observed temperature of IRC +10216 was also compared directly with BTL 7 m observations (Kwan and Linke 1982), both observations deconvolved with a Gaussian model for the brightness distribution of the source, with a 2.1 FWHM (Ulich and Haas 1976), obtaining $\eta = 0.84 \pm 0.05$. Since the value of 0.82 obtained from diffraction theory and the measured antenna pattern is in excellent agreement with that obtained observationally, we adopt it here.

The antenna temperature corrected for beam efficiency, $T_A^*/\eta \equiv T_R$, is equal to the radiation temperature of a uniform source that just fills the main beam to the first null of the antenna pattern. It differs from the definition given by Kutner and Ulich (1981), T_R^*, in that it includes corrections for losses in the near sidelobes. For the Chile Telescope, $T_R(\mathrm{Ch}) = 1.08 T_R^*$.

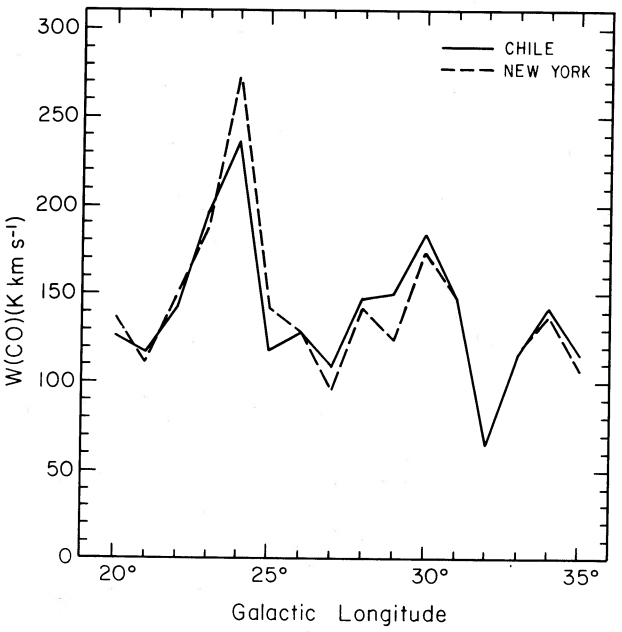

FIG. 19

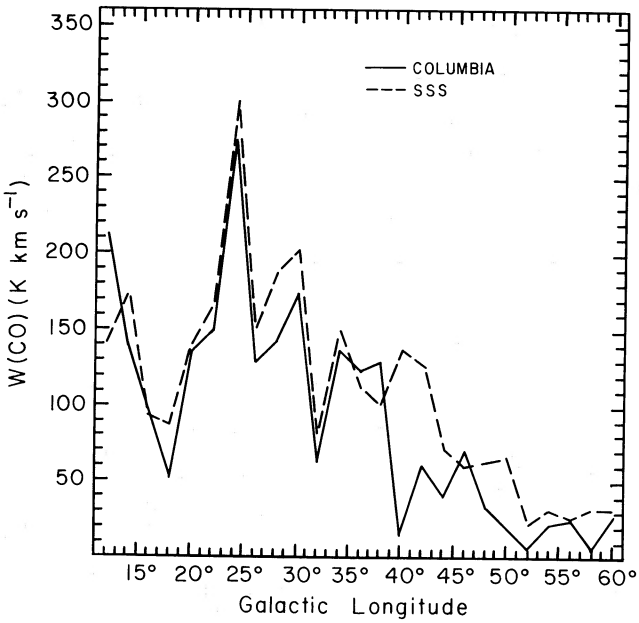

FIG. 20

FIG. 19.—Comparison of the calibrations of the Southern and Northern Columbia CO Surveys. Velocity integrated radiation temperatures, W(CO) (§ II), were compared for 16 positions in the first Galactic quadrant, at $b^\circ = 0$, observed with the Chile Telescope and the New York Telescope.

FIG. 20.—Comparison of the calibrations of the Columbia Northern Survey and of the Stony Brook/Massachusetts Survey. Velocity integrated radiation temperatures, W(CO), were compared for 25 positions at $b^\circ = 0$ in the first Galactic quadrant.

II. COMPARISON WITH CALIBRATIONS OF THE COLUMBIA NORTHERN SURVEYS

Because the Chile and the New York telescopes are so similar, their calibrations relative to each other can be more accurately determined than those relative to larger telescopes, such as the BTL 7 m or FCRAO 14 m. The relative calibration of the Southern and Northern Surveys was obtained by observing with the Chile Telescope 16 positions in the first Galactic quadrant, at $b = 0°$, every degree in longitude from 20° to 35°, and comparing the velocity-integrated intensities, $\int T_R(\mathrm{Ch})dv$, with those from the Northern Survey, $\int T_R(N)dv$, obtaining $\langle \int T_R(\mathrm{Ch})dv \rangle / \langle \int T_R(N)dv \rangle = 1.29 \pm 0.2$, a result confirmed independently by a comparison of observations of Orion made with both instruments. The ratio can be decomposed as $1.29 \approx 1.13 \times 1.14$. The first factor results from an improved estimate of the oxygen opacities used in the atmospheric model; the second is due largely to uncertainties in the difficult estimation of the spillover of the pyramidal feed horn around the secondary of the New York Telescope in 1977–1979, when the Northern Survey was carried out.

The Wide-Latitude Northern Survey, used together with H I and γ-ray data by Bloemen *et al.* (1986) to derive the $N(H_2)$-to-W_{CO} ratio, was made in 1981–1983 using the New York Telescope in a slightly different configuration from that used for the Northern Survey. The ratio of $T_R(\mathrm{Ch})$ to T_R from the Wide Survey was derived from a comparison of observations of Orion and W51 made with the Chile Telescope and with the New York Telescope (in the Wide Survey configuration): $T_R(\mathrm{Ch})/T_R = 1.22 \pm 0.04$. This ratio can be decomposed as $1.22 = 1.13 \times 1.08$, the factors derived, respectively, from improvements in the atmospheric model and in the estimation of the beam efficiency of the New York Telescope in the Wide Survey configuration. For the reasons given in § II, all present data have been scaled to agree with the Wide Survey calibration. Figure 19 compares the New York and Chile observations, both in the Wide Survey scale; Figure 20 compares data from the Northern Survey with data from the Stony Brook/Massachusetts Survey. The latter comparison has also been made independently by Sanders *et al.* (1986), who obtain the same results when their recalibration of -10% with respect to SSS and our difference of $+6\%$ with the Northern Survey scale both are taken into account.

APPENDIX B

STATISTICAL ANALYSIS OF THE DATA

I. THE AXISYMMETRIC MODEL

We assume the number of H_2 molecules in a volume element d^3x of the Galaxy is a random variable with expectation value $n^m(\boldsymbol{x}; \Lambda)d^3x$, where $n^m(\boldsymbol{x}; \Lambda)$, the model H_2 number density, is a smooth (on a scale $\lesssim 0.5$ kpc) function of position $\boldsymbol{x}$ and depends on S model parameters $\Lambda = (\lambda_1, \lambda_2, \ldots, \lambda_j, \ldots, \lambda_S)$. A set of density measurements would allow the adjustment of the model parameters according to some best-fit criterion; however, owing to the twofold distance ambiguity, it is not possible to measure directly the density at a given position. To circumvent this limitation, $n^m(\boldsymbol{x}; \Lambda)$ is chosen to be axisymmetric, i.e., $n^m(\boldsymbol{x}; \Lambda) \equiv n^m(R, z; \Lambda)$; an array of model spectra, $T^m(l, b, v; \Lambda)$, is computed from $n^m(R, z; \Lambda)$, and the parameters Λ adjusted through a maximum likelihood analysis to yield a best fit of modeled to observed spectra.

The model radiation temperature integrated over a channel width Δv can be expressed as a function of a model emissivity, $\epsilon^m(R, z; \Lambda)$, and, using equation (1), of the model number density:

$$T_R^m(l, b, v; \Lambda)\Delta v = \left[\int_{\Delta s \text{ near}} \epsilon^m(R, z; \Lambda)ds + \int_{\Delta s \text{ far}} \epsilon^m(R, z; \Lambda)ds \right] ,$$

$$\approx (1/X)[n^m(R^\dagger, z^{\text{near}}; \Lambda) + n^m(R^\dagger, z^{\text{far}}; \Lambda)]\Delta s , \tag{B1}$$

where Δs is the segment of line of sight corresponding to Δv and $R^\dagger$ is obtained by using Burton and Gordon's (1978) rotation curve:

$$R^\dagger \equiv [R(l, v + \Delta v/2) + R(l, v - \Delta v/2)]/2 . \tag{B2}$$

The CO emissivity (eq. [2]) is assumed to be a Gaussian function of z, with amplitude ϵ_0, displacement from the conventional Galactic plane z_0, and half-width $z_{1/2}$, all functions of R. To simplify the numerical computation, the Galaxy is divided into concentric rings of width $\Delta R = 0.5$ kpc, with ϵ_0, z_0, and $z_{1/2}$ constant for each ring; in this way, the problem is reduced to a series of independent maximum likelihood three-parameter fits.

II. MAXIMUM LIKELIHOOD ANALYSIS

For each ring, the likelihood function, L, to be maximized is given by

$$L = -\sum_i \log P[T_i; T^*(y_i; \Lambda)] , \tag{B3}$$

where $P[T_i; T^*(y_i; \Lambda)]$ is the probability of measuring an antenna temperature T_i at $y_i = (l_i, b_i, v_i)$, when the expectation value is $T^*(y_i; \Lambda)$ and the sum extends over all the data contributing to the ring. The parameters $\Lambda = (\lambda_1, \lambda_2, \lambda_3) \equiv (\epsilon_0, z_0, z_{1/2})$ are determined from the maximum likelihood conditions,

$$\partial L/\partial \lambda_j = 0, \qquad j = 1, 2, 3 . \tag{B4}$$

To solve equation (B4) the probability function $P[T_i; T^*(y_i, \Lambda)]$ is needed. Two terms contribute to the measured temperatures T_i, i.e., $T_i = T_n + T_{Ri}$: the first, the instrumental background noise, is Gaussian distributed, with an expectation value $T_n^* = 0$ K and variance T_{rms}^2; the second, T_{Ri}, the radiation temperature of the source averaged over the beam and over the channel, has an

expectation value $T_R^m(y_i, \Lambda)$ and an unknown distribution. To estimate the distribution of T_{Ri}, we assume that the gas is organized into a few large, beam-filling molecular complexes, so that T_{Ri} is proportional to the number of clouds, N_i, intercepted by the segment of line of sight that corresponds to one spectrometer channel:

$$T_{Ri} = N_i T_0 = [N_i^{\rm near} + N_i^{\rm far}] T_0 \,. \tag{B5}$$

The expectation values are similarly related:

$$T^m(y_i; \Lambda) = N_i^* T_0 \,. \tag{B6}$$

For simplicity, we assumed the radiation temperature of a cloud, T_0, to be constant, and used the value of 1 K, although no appreciable changes in the results were observed using values from 0.1 K to 10 K.

The number of clouds N_i intercepted by the segment of line of sight is approximately Poisson distributed, so its variance, $\sigma_{N_i}^2$, is equal to its expectation value, N_i^*. The variance in T_{Ri}, σ_{Ri}^2, is then given by

$$\begin{aligned} \sigma_{Ri}^2 &= T_0^2 \sigma_{N_i}^2 \\ &= T_0^2 N_i^* \\ &= T_0 T^m(y_i; \Lambda) \,. \end{aligned} \tag{B7}$$

The expectation value and the variance of the temperature probability distribution are then

$$\begin{aligned} T^*(y_i; \Lambda) &= T_n^* + T^m(y_i; \Lambda) = T^m(y_i; \Lambda) \\ \sigma_i^2 &= T_{\rm rms}^2 + T_0 T^m(y_i; \Lambda) \,, \end{aligned} \tag{B8}$$

and its functional form is the convolution of a Gaussian and a Poisson distribution. In this case, the maximum likelihood conditions (B4) are very difficult to solve analytically but can be approximated by generalized least-squares conditions in which each datum is properly weighted by the inverse of its variance (Janossy 1965); equation (B4) becomes

$$\sum_i (1/\sigma_i^2)(\partial/\partial\lambda_j)\{[T_i - T^m(y_i; \Lambda)]^2\} = 0 \,. \tag{B9}$$

Correct results are obtained by an iterative process in which the variation of the weights, $W = 1/\sigma_i^2$, with respect to the parameters Λ is neglected when minimizing the quadratic expression (Janossy 1965); at each iteration, however, the weights are revaluated using the values for Λ obtained in the previous step. The uniqueness of the convergence was checked by fitting the model to small fractions of the data, randomly chosen, and in every case obtaining the same solution within the error bars.

The analysis as described assumes that each datum, i.e., each line of sight and channel, is statistically independent. Because data across the face of a cloud are highly correlated, this straightforward analysis will lead to underestimation of errors of the fitted parameters. To correct for this effect, the formal errors of the least-squares fit in the ring at radius R were multiplied by a factor $[N(R)]^{1/2}$, where $N(R)$ is the number of resolution elements included in a typical molecular cloud; to find $N(R)$ we assumed a cloud of average size (50 pc) with a line of 6 km s^{-1}, and placed it at the average solar distance of the ring. The correction factors ranged from ~ 6 at $R = 2.5$ kpc to ~ 10 at $R = 8.5$ kpc, for a velocity resolution of 1.3 km s^{-1} and a sampling interval of 0°.125.

APPENDIX C

COMPARISON OF PRESENT AND PREVIOUS STATISTICAL ANALYSES OF THE DATA

I. OLD COLUMBIA METHOD

Our present and previous axisymmetric analyses (Cohen and Thaddeus 1977; Thaddeus and Dame 1984) differ primarily in the weights used to fit the model to the data. As described in Appendix B, in the present analysis the weight assigned each datum differs according to the variance in its probability:

$$W = 1/\sigma^2 = 1/(T_{\rm rms}^2 + T_0 T^m) \,. \tag{C1}$$

Previously, the uncertainties were assumed to come only from constant instrumental noise, i.e., the variance in the antenna temperature was $\sigma_{\rm old}^2 = T_{\rm rms}^2$, the weight assigned to each datum in the fit being

$$W_{\rm old} = 1/\sigma_{\rm old}^2 = 1/T_{\rm rms}^2 \,. \tag{C2}$$

The weighting led to an underestimation in the CO emissivities of $\sim 20\%$.

II. SSS METHOD

To adjust the parameters of the axisymmetric model, SSS used the "observed emissivity,"

$$J(l, B, v) \equiv (\Delta v/\Delta s) T(l, b, v) \,, \tag{C3}$$

as the variable for a least-squares fit performed independently for every ring and longitude, all the data equally weighted in the fit; the resultant parameters $\epsilon_0(R, l)$, $z_{1/2}(R, l)$, and $z_0(R, l)$ were averaged over all longitudes. By assigning equal weights to the data, statistical fluctuations in the number of clouds sampled in each line of sight and velocity interval were neglected. Further, when averaging over longitude, equal weights were assigned to lines of sight with very different sampled path lengths.

Sanders (1981) has argued that by fitting the data separately at each longitude it is possible to follow azimuthal warps in the Galaxy. Such a scheme is defective, since, owing to the distance ambiguity, two azimuths contribute to each datum: for example, if the Galaxy were warped towards positive latitudes in the near side and toward negative latitudes in the far side, the results of a fit made at a particular longitude would yield a displacement near zero.

III. REDUCTION TO $b = 0°$

The effect of the different weightings can be seen more easily if the data are restricted to the Galactic equator. In this case, z_0 and $z_{1/2}$ cannot be determined, but ϵ_0 can be obtained algebraically:

$$\epsilon_0^{(1)} = \tfrac{1}{2}\Delta v\langle T\Delta s\rangle/\langle\Delta s^2\rangle \quad \text{(Old Columbia)},$$

$$\epsilon_0^{(2)} = \tfrac{1}{2}\Delta v\langle T/\Delta s\rangle \quad \text{(SSS)},$$

and

$$\epsilon_0^{(3)} = \tfrac{1}{2}\Delta v\langle T\rangle/\langle\Delta s\rangle \quad \text{(this work)},$$

where the average is taken over all spectrometer channels with emission from a particular ring and on the assumption that, for $\epsilon_0^{(3)}$, $T_{\rm rms}^2 \ll T_0\, T^m$ at $=0°$. Since the differential quantity dv/ds along the line of sight is particularly small near the subcentral points, our old method weights most heavily the confused tangential regions, with a large Δs, where the distances are most uncertain.

The SSS method assigns equal weights to different spatial regions, even though the path length that corresponds to a single channel, Δs, varies considerably. For example, at $R \approx 5$ kpc, Δs varies from as little as 100 pc near the solar circle to up to 450 pc at a distance of 8.7 kpc, near the tangent point. The very high values of the emissivity in the northern molecular ring obtained by SSS seem partly to result from overweighting the emission from the Scutum spiral arm (Dame 1983), whose largest molecular complexes are far from the tangent of the ring.

Finally, our present method reduces at $b = 0°$ to the formula used by Burton *et al.* (1975), which correctly predicts the CO luminosities, and hence the gas column densities.

APPENDIX D

EFFECT OF THE NEW IAU GALACTIC CONSTANTS

It is important to consider what effect on the present analysis a change in the Galactic constants $R_\odot$ and $\theta_\odot$ (here, $R_\odot = 10$ kpc, $\theta_\odot = 250$ km s^{-1}) would work, in particular a change to the new values ($R_\odot = 8.5$ kpc, $\theta_\odot = 220$ km s^{-1}) approved by the 1985 IAU General Assembly in Delhi.

As pointed out by Kerr and Lynden-Bell (1986), kinematic distances inside the solar circle derived with a rotation curve from radial velocity measurements scale directly with $R_\odot$. Further, such distances are insensitive to $\theta_\odot$, because the value of $\theta_\odot$ assumed for the rotation curve drops when the curve is used to derive kinematic distances. As a consequence, the mean position of the CO layer relative to the Galactic plane, $z_0(R)$, and the half-width at half-maximum of the CO distribution, $z_{1/2}(R)$, which depend linearly on those distances, also will scale directly with $R_\odot$. The CO emissivities, hence the gas densities, will scale inversely with $R_\odot$, because the product of both the emissivity and the path length associated with a resolution element in a given line of sight and at a given radial velocity is proportional to the line intensity measured in the corresponding spectrometer channel, which is a model-independent quantity.

If we use the values recommended by the IAU for the Galactic constants, then R, $z_0(R)$, and $z_{1/2}(R)$ scale down by a factor of 0.85; the emissivity $\epsilon_0(R)$ and the number density $n_0(R)$ scales up by $1.18(= 0.85^{-1})$; H_2 masses scale down by $0.72(= 0.85^2)$; and the H_2 face-on surface density, $\sigma(R)$, remains unchanged. So long as the H_2 and the H I follow the same kinematics, neither the present CO-to-H_2 conversion factor nor the derived H_2/H I ratio are affected by such a change.

REFERENCES

Bloemen, J. B. G. M., *et al.* 1986, *Astr. Ap.*, **154**, 25.
Bronfman, L. 1986, Ph.D. thesis, Columbia University.
Bronfman, L., Cohen, R. S., Thaddeus, P., and Alvarez, H. 1985, in *IAU Symposium 106, The Milky Way*, ed. H. Van Woerden, R. J. Allen, and W. N. Burton (Dordrecht: Reidel), p. 331.
Burton, W. B., and Gordon, M. A. 1978, *Astr. Ap.*, **63**, 7.
Burton, W. B., Gordon, M. A., Bania, T. M., and Lockman, F. J. 1975, *Ap. J.*, **202**, 30.
Cohen, R. S. 1978, Ph.D. thesis, Columbia University; NASA Tech. Memo. 78071.
Cohen, R. S., Cong, H., Dame, T. M., and Thaddeus, P. 1980, *Ap. J. (Letters)*, **217**, L155.
Cohen, R. S., Dame, T. M., and Thaddeus, P. 1986, *Ap. J. Suppl.*, **60**, 695.
Cohen, R. S., Grabelsky, D. A., May, J., Bronfman, L., Alvarez, H., and Thaddeus, P. 1985, *Ap. J. (Letters)*, **290**, L15.
Cohen, R. S., and Thaddeus, P. 1977, *Ap. J. (Letters)*, **217**, L155.
Cohen, R. S., Thaddeus, P., and Bronfman, L. 1985, in *IAU Symposium 106, The Milky Way*, ed. H. Van Woerden, R. J. Allen, and W. B. Burton (Dordrecht: Reidel), p. 199.
Cohen, R. S., Tomasevich, G. R., and Thaddeus, P. 1979, in *IAU Symposium 84, The Large-Scale Characteristics of the Galaxy*, ed. W. B. Burton (Dordrecht: Reidel), p. 53.
Courtès, G., Georgelin, Y. P., Georgelin, Y. M., and Monnet, G. 1970, in *IAU Symposium 38, The Spiral Structure of Our Galaxy*, ed. W. Becker and T. Contopoulos (Dordrecht: Reidel), p. 209.
Dame, T. M. 1983, Ph.D. thesis, Columbia University; NASA Tech. Rept. 2288.
Dame, T. M., Elmegreen, B. G., Cohen, R. S., and Thaddeus, P. 1986, *Ap. J.*, **305**, 892.
Dame, T. M., and Thaddeus, P. 1985, *Ap. J.*, **297**, 751.
Dame, T. M., *et al.* 1987, *Ap. J.*, submitted.
Georgelin, Y. M., and Georgelin, Y. P. 1976, *Astr. Ap.*, **49**, 57.

Grabelsky, D. A., *et al.* 1987, *Ap. J.*, **315**, 122.
Henderson, A. P., Jackson, P. D., and Kerr, F. J. 1982, *Ap. J.*, **263**, 116.
Janossy, L. 1965, *Theory and Practice of the Evaluation of Measurements* (Oxford: Oxford University Press).
Kerr, F. J. 1970, in *IAU Symposium 38, The Spiral Structure of Our Galaxy*, ed. W. Becker and T. Contopoulos (Dordrecht: Reidel), p. 95.
Kerr, F. J., and Lynden-Bell, D. 1986, *M.N.R.A.S.*, **221**, 1023.
Kutner, M. L., and Ulich, B. L. 1981, *Ap. J.*, **250**, 341.
Kwan, J., and Hill, F. 1977, *Ap. J.*, **215**, 781.
Kwan, J., and Linke, R. 1982, *Ap. J.*, **254**, 587.
Lebrun, F., *et al.* 1983, *Ap. J.*, **274**, 231.
Robinson, B. J., *et al.* 1984, *Ap. J.* (*Letters*), **283**, L31.
Rougoor, G. W., and Oort, J. H. 1960, *Proc. Nat. Acad. Sci.*, **46**, 1.
Sanders, D. B. 1981, Ph.D. thesis, State University of New York at Stony Brook.
Sanders, D. B., Clemens, D. P., Scoville, N. Z., and Solomon, P. M. 1986, *Ap. J. Suppl.*, **60**, 1.
Sanders, D. B., Solomon, P. M., and Scoville, N. Z. 1984, *Ap. J.*, **276**, 182 (SSS).
Scoville, N. Z., and Solomon, P. M. 1975, *Ap. J.* (*Letters*), **199**, L105.
Solomon, P. M., and Sanders, D. B. 1980, in *Giant Molecular Clouds in the Galaxy*, ed. P. M. Solomon and M. G. Edmunds (Oxford: Pergamon), p. 41.
Solomon, P. M., Sanders, D. B., and Scoville, N. Z. 1979, in *IAU Symposium 84, The Large-Scale Characteristics of the Galaxy*, ed. W. B. Burton (Dordrecht: Reidel), p. 35.
Solomon, P. M., Scoville, N. Z., and Sanders, D. B. 1979, *Ap. J.* (*Letters*), **232**, L89.
Thaddeus, P., and Dame, T. M. 1984, *Proc. Workshop on Star Formation*, in *Occasional Reports of Royal Observatory, Edinburgh*, ed. R. Wolstencroft, Vol. **13**, p. 15.
Ulich, B. L., and Haas, R. W. 1976, *Ap. J. Suppl.*, **30**, 247.
Weaver, H. 1970, in *IAU Symposium 38, The Spiral Structure of Our Galaxy*, ed. W. Becker and T. Contopoulos (Dordrecht: Reidel), p. 126.

H. ALVAREZ, L. BRONFMAN, and J. MAY: Departmento de Astronomía, Universidad de Chile, Casilla 36-D, Santiago, Chile

R. S. COHEN: 51 Seventh Avenue, Apt. 1, Brooklyn, NY 11217

P. THADDEUS: Harvard-Smithsonian Center for Astrophysics, 60 Garden Street, Cambridge, MA 02138